

Structural, Antimicrobial and *in Silico* Studies of Some Schiff Bases of Trans-paramethoxycinnamaldehyde Derivatives

G. U. Kaior, N. J. Nwodo, U. S. Oruma, A. Ibezim, A. E. Ochonogor, K. K. Onyia and N. L. Obasi^{1*}

Received 29 May 2020/Accepted 29 July 2020/Published online: 30 July 2020

Abstract Three Schiff bases viz; 3,5-bis[(E)-[(2E)-3-(4-methoxyphenyl)prop-2-en-1-ylidene]benzoic acid (3,5-DA), 2-[(E)-[(2E)-3-(4-methoxyphenyl)prop-2-en-1-ylidene]amino]phenol (OAP) and [3-(4-methoxy-phenyl)-allylidene]-[2-(2-{2-[3-(4-methoxy-phenyl)-allylideneamino]-ethoxy}-ethoxy)-ethyl]-amine (TPMC/DDE) are reported. The Schiff bases were synthesized from the condensation reaction of trans-paramethoxycinnamaldehyde and the primary amines (3,5-diaminobenzoic acid, 2-aminophenol and 1,8-diamino-3,6-dioxaoctane respectively), in dry methanol. The synthesized Schiff bases were characterized using UV-Visible, Fourier transform infrared (FTIR), ¹H, and ¹³C NMR spectroscopies. The *In vitro* antimicrobial screening of the Schiff bases were carried out on gram-positive bacteria: (*Staphylococcus aureus* and *Bacillus subtilis*) and gram-negative bacteria: (*Pseudomonas aeruginosa*, and *Escherichia coli* strain13) and against the fungi, *Aspergillus niger* and *Candida albicans* using the agar well diffusion method. The ligands 3,5-DA and OAP only showed activity against the fungus, *Candida albicans* with inhibition zone diameter (IZD) of 10 mm and minimum inhibitory concentrations (MIC) of 5.0 mg/mL and 3.0 mg/mL respectively. The ligand, TPMC/DDE also showed varying activity against the bacteria, *Pseudomonas aeruginosa* with an IZD of 8.0 mm and MIC of 7.5 mg/mL while *Escherichia coli* displayed inhibition with an IZD of 10.0 mm and MIC of 1.9 mg/mL. According to molecular docking studies, the binding affinity of the compounds towards two validated antibiotic and antifungal drug targets (DD-transpeptidase-DDPT and N-myristoyl transferase-NMT) were in agreement to their observed *in vitro* antimicrobial activities. Moreover, their retrieved binding poses explained intermolecular forces behind the interactions that exist between the proteins and the ligands, a knowledge which is very useful in structural modification for activity optimization.

Key Words: *Trans-paramethoxycinnamaldehyde*; 2,4-diaminobenzoic acid; 2-aminophenol; 1,8-diamino-3,6-dioxaoctane, binding poses.

G. U. Kaior

Department of Pure and Industrial Chemistry
University of Nigeria, Nsukka, Enugu State,
Nigeria

Email: gracykaior@yahoo.com

Orcid id: 0000-0001-5269-4102

N. J. Nwodo

Department of Pharmaceutical and Medicinal
Chemistry, University of Nigeria, Nsukka,
Enugu State, Nigeria

Email: ngozi.nwodo@unn.edu.ng

Orcid id: 0000-0001-9914-6402

U. S. Oruma,

Department of Pure and Industrial Chemistry
University of Nigeria, Nsukka,
Enugu State, Nigeria

Email: susan.oruma@unn.edu.ng

Orcid id: 0000-0002-9226-2512

A. Ibezim

Department of Pure and Industrial Chemistry
University of Nigeria, Nsukka,
Enugu State, Nigeria

Email: akachukwu.ibezi@unn.edu.ng

Orcid id: 0000-0003-1620-5716

A. E. Ochonogor

Department of Pure and Industrial Chemistry
University of Nigeria, Nsukka,
Enugu State, Nigeria

Email: alfred.ochonogor@unn.edu.ng

Orcid id: 0000-0001-7629-9668

K. K. Onyia

Department of Pure and Industrial Chemistry
University of Nigeria, Nsukka,
Enugu State, Nigeria

Email: kenechi.onyia@unn.edu.ng

Orcid id: 0000-0002-9682-5618

Nnamdi L. Obasi*

Department of Pure and Industrial Chemistry
University of Nigeria, Nsukka,
Enugu State, Nigeria

Email: nnamdi.obasi@unn.edu.ng

Orcid id: [0000-0001-9310-0825](https://orcid.org/0000-0001-9310-0825)

1.0 Introduction

Several Schiff bases have been reported to possess remarkable antibacterial, antifungal, anticancer and diuretic activities (Ahamad *et al.*, 2010; Finar, 2006; Golcu *et al.*, 2005; Prakash and Adhikari, 2011; Mokhles *et al.*, 2014; Mostafa *et al.*, 2012; Vogel, 1989). They have wide applications in food and dye industries, in analytical chemistry, as catalysts, and as agrochemicals (Mohammed and Salatheddi, 2011; Raman *et al.*, 2004; Schmid, 1999). Schiff bases obtained from amino acids could be used in explaining transamination reactions in living systems (Andrew *et al.*, 1992; Iihan *et al.*, 2007). Schiff bases are studied widely due to their synthetic flexibility, selectivity and sensitivity towards the central metal atom, structural similarities with natural biological compounds and also due to the presence of an azomethine group (-N=CH-) (Pallavi *et al.*, 2014). Imine or azomethine groups are present in various naturally derived and non-natural compounds. The imine group present in such compounds has been shown to be critical to their biological activity (Bansade, 2012). Schiff bases having oxygen and nitrogen atoms possess structural liability and are sensitive to molecular environment (Ikechukwu and Peter, 2015; Mangaiyarkkara and Arul, 2014; Mashaly *et al.*, 2004; Rhohini and Arul, 2014; Sobola *et al.*, 2014; Suresh and Prakash, 2011; Thomas *et al.*, 2011). Examples of Schiff bases that contain oxygen and nitrogen atoms are those derived from 4-methoxycinnamaldehyde, salicylaldehyde, amino acids and hydrazones.

Potato and oil of tarragon (*Artemisia dracunculus*) are known sources of methoxycinnamaldehyde (Yannai, 2004). It is generally used as a flavouring agent in food additives (Arun *et al.*, 2002). 4-methoxycinnamaldehyde has been reported to be an inhibitor for the human respiratory syncytial virus in a human larynx carcinoma cell line (Wang *et al.*, 2009). Cinnamon essential oil (which contains paramethoxycinnamaldehyde) has also been found to exhibit a preventive effect on lipid oxidation of vegetable oils (Keshvari *et al.*, 2013). The work by Kong *et al.* (2007) indicates that cassia, cinnamon oil

compounds and related compounds could be useful as potential nematocides for *Bursaphelenchus xylophilus* (Nematoda: Parasitaphelenchidae) (Kong *et al.*, 2007). The work by Ooi *et al.* (2006), showed that *cinnamomum cassia* comprises of 85% cinnamaldehyde which is effective in inhibiting the growth of bacteria, fungi and dermatophytes (Ooi *et al.*, 2006). A search through literature revealed that cinnamaldehyde derivatives possess significant antibacterial (Obasi *et al.*, 2017; Seelolla *et al.*, 2014), antifungal (Obasi *et al.*, 2017; Yuan *et al.*, 2015) and antioxidant (Seelolla *et al.*, 2014) properties.

In view of the need to develop new and more potent antimicrobial drugs with low toxicity, we synthesized *trans*-paramethoxycinnamaldehyde derivatives using 3,5-diaminobenzoic acid, 2-aminophenol and 1,8-diamino-3,6-dioxaoctane, respectively. The binding affinity of the compounds towards two validated antibiotic and antifungal drug targets (DD-transpeptidase – DDPT and N-myristoyl transferase - NMT), respectively according to molecular docking studies, also stimulated our interest to investigate the *in vitro* antimicrobial activities of the Schiff bases. We have patented these compounds in Nigeria with patent No: NG/P/2018/269.

2.0 Materials and Methods

2.1 Reagents and Apparatus

The chemicals used were of analytical grade and they were used without further purification. The syntheses of the compounds were carried out using procedures reported by Obasi *et al.* (2016). The melting points of the Schiff bases were determined using Fisher-Johns Melting point apparatus (Japan), UV-Visible spectra were obtained on UV-1800 UV-VIS Spectrophotometer (SHIMADZU) at the National Research Institute for Chemical Technology (NARICT), Zaria, Kaduna State, Nigeria. Infrared spectra were recorded on a PerkinElmer (Waltham, MA) FTIR spectrophotometer. Elemental analyses were performed on a LECO-CHNS-932 Analyser. The NMR spectra were recorded on a Bruker 400 MHz Avance-III HD spectrometer, Bruker Biospin GmbH, with broad band decoupling of ^1H at 400.25 MHz and ^{13}C at 100.65 MHz. Chemical shifts (δ) are given in ppm and referenced to tetramethylsilane (^1H , ^{13}C).

2.2 Antimicrobial Screening

The antibacterial screening was carried out at the Faculty of Pharmaceutical Sciences, University of Nigeria, Nsukka. The compounds were screened *in*



vitro against the gram-positive bacteria (*Staphylococcus aureus* and *Bacillus subtilis*) and gram-negative bacteria (*Pseudomonas aeruginosa*, and *Escherichia coli* strain 13) and against the fungi, *Aspergillus niger* and *Candida albicans* using the conventional drugs, ciprofloxacin (an antibacterial) and ketoconazole (an antifungal drug) as standards for the agar well diffusion screening method described by Chah *et al.* (2006). The minimum inhibitory concentrations (MIC) of the test compounds were determined using the agar dilution method as described by Ojo *et al.* (2007).

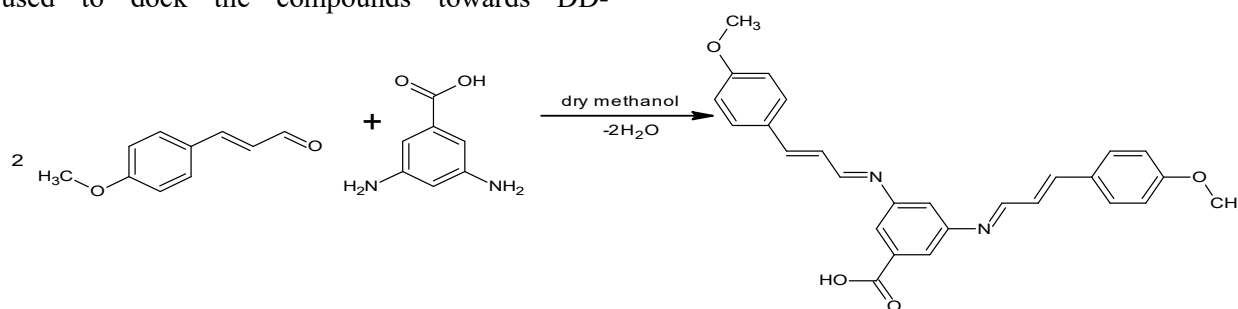
2.3 Molecular Simulation

The X-ray crystal structure of the DD-transpeptidase (DDPT) and N-myristoyl transferase (NMT) in complex with their co-crystallized inhibitors were retrieved from the protein databank (Berman *et al.*, 2000) and treated using molecular operating environment (MOE) as follows: the co-crystallized water molecules and small molecules were deleted. The retained protein-ligand complexes were protonated using the protonate 3D procedure implemented in Molecular Operating Environment (MOE) (2010). To remove atomic clashes, energy minimization was carried out on the protonated complexes using the Merck Molecular Force Field (MMFF94) (Halgren, 1996) until a gradient of 0.001 kcal/mol was attained. Chemical structures (3D) were generated using the graphical user interface (GUI) of the MOE software. MOE Dock tool was used to dock the compounds towards DD-

transpeptidase (DDTP) by; carrying out conformational analysis of the ligands, using Triangle Matcher Placement method to make poses and estimating the free energy of binding of the ligands from a given pose using London dG scoring function.

2.4 Synthesis of 3,5-Bis[(E)-[(2E)-3-(4-methoxyphenyl)prop-2-en-1-ylidene]amino]benzoic Acid (3,5-DA)

To a solution of *trans-p*-methoxycinnamaldehyde (0.81 g, 5 mmol) in dry methanol (10 mL) was added a solution of 3,5-diaminobenzoic acid (0.76 g, 5 mmol) in dry methanol (15 mL). The solution was heated at reflux for 1 hour at 70 °C during which a yellow solid was formed. It was filtered and recrystallized from methanol and stored in a desiccator. The yield was 93.18 % (1.025 g) and melting range was 168 – 170 °C. UV (λ_{\max} nm) (DMF): 389.0, 459.0; IR (ν cm⁻¹): 3504 (br), 3122 (s), 2981 (s), 2861 (s), 1942 (s), 1618 (s), 1613 (s), 1357 (s), 1246 (s); ¹H NMR (δ ppm): 2.16 (3H, s), 5.99 (1H, d), 6.03 (1H, d), 6.33 (1H, s), 9.60 (1H, d), 6.81-7.66 (7H, m); ¹³C NMR (δ ppm): 55.97, 115.60, 151.0, 118.01, 127.23, 127.23, 129.05, 130.05, 130.10, 130.62, 134.50, 159.25, 174.24; Anal. calcd. For C₂₇H₂₄N₂O₄ = 440.00 g/mol, %C = 73.6, %H = 5.5, %N = 6.3, Found %C = 73.4, %H = 5.8, %N = 5.8. (See Scheme 1, the ¹H and ¹³C NMR spectra of 3,5-DA are shown in Appendices 1 and 2 respectively).



Scheme 1: Synthesis of 3,5-bis[(E)-[(2E)-3-(4-methoxyphenyl)prop-2-en-1-ylidene]amino]benzoic acid (3,5-DA).

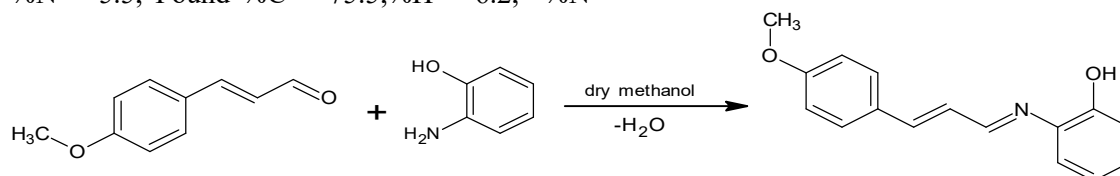
2.5 Synthesis of 2-[(E)-[(2E)-3-(4-Methoxyphenyl)prop-2-en-1-ylidene]amino]phenol (OAP)

To a solution of *trans-p*-methoxycinnamaldehyde (1.62 g, 10 mmol) in dry methanol (15 mL) was added a solution of *o*-aminophenol (1.09 g, 10 mmol) in dry methanol (18 mL). This was heated at reflux for about 1 h at 70 °C during which yellow crystals were formed. The crystals were filtered,

recrystallized from methanol and stored in a desiccator. The yield was 68.97 % (1.745 g) and melting point ranged from 197 – 199 °C. UV (λ_{\max} nm) (DMF), 429.0; IR (ν cm⁻¹): 3690 (br), 3117 (s), 3003 (s), 2814 (s), 1637 (s), 1424 (s), 1357 (s); ¹H NMR (δ ppm): 3.86 (3H, s), 4.96 (1H, s), 6.82 (1H, t), 6.93 (1H, d), 9.62 (1H, d), 8.39 (1H, d), 6.98-7.59 (8H, m); ¹³C NMR (δ ppm): 55.91, 115.49, 116.94, 123.36, 126.17, 129.86, 130.28, 130.15, 143.75,



143.83, 145.70, 157.88, 161.79, 162.64; Anal. calcd. For $C_{16}H_{15}NO_2 = 253$ g/mol, %C = 75.9, %H = 5.9, %N = 5.5, Found %C = 75.5, %H = 6.2, %N = 5.6. (See Scheme 2, the 1H and ^{13}C NMR spectra of OAP are shown in Appendices 3 and 4 respectively).

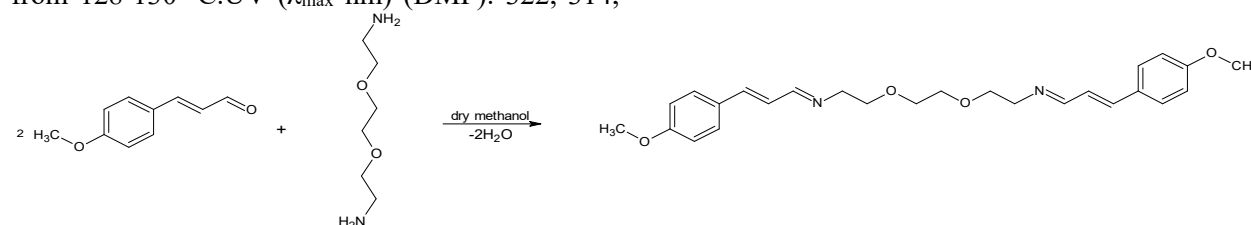


Scheme 2: Synthesis of 2-[(E)-[(2E)-3-(4-methoxyphenyl)prop-2-en-1-ylidene]amino]phenol (OAP).

2.6 Synthesis of [3-(4-Methoxy-phenyl)-allylidene]-[2-(2-{2-[3-(4-methoxy-phenyl)-allylideneamino]-ethoxy}-ethoxy)-ethyl]-amine (TPMC/DDE)

To a solution of *trans-p*-methoxycinnamaldehyde (3.20 g; 20 mmol) in dry methanol (20 mL) was added 1,8-diamino-3,6-dioxaoctane (1.48g; 10 mmol). The mixture was heated at reflux for 3 h at 75 °C over water bath with constant stirring, during which a Pale pink powder was formed which was collected and recrystallized in hot methanol. The yield was 71.00 % (3.05 g) and melting point ranged from 128-130 °C. UV (λ_{max} nm) (DMF): 322, 314,

310; IR (ν cm^{-1}): 3182(s), 2852(s), 3182 (s), 2852 (s), 1783 (s), 1632 (s), 1598 (s), 1303 (s), 1251 (s); 1H NMR (δ ppm): 2.09 (3H, s), 3.55-3.63 (4H, m), 3.76 (4H,s), 6.65 (1H,d), 6.69 (1H,d), 6.87 (1H,t), 6.98 (2H,d), 7.42 (2H,d), 7.94 (2H, d); ^{13}C NMR (δ ppm): 55.87, 60.98, 71.57, 71.62, 115.43, 125.35, 129.59, 130.16, 144.86, 162.50, 167.68; Anal. calcd. For $C_{26}H_{32}N_2O_4 = 436.31$ g/mol, %C = 71.60, %H = 7.30, %N = 6.40, Found %C = 70.90, %H = 7.70, %N = 6.00. (See Scheme 3, the 1H and ^{13}C NMR spectra of TPMC/DDE are shown in Appendices 5 and 6 respectively).



Scheme 3: Synthesis of [3-(4-Methoxy-phenyl)-allylidene]-[2-(2-{2-[3-(4-methoxy-phenyl)-allylideneamino]-ethoxy}-ethoxy)-ethyl]-amine (TPMC/DDE).

3.0 Results and Discussion

The reaction of *trans-p*-methoxycinnamaldehyde with three different classes of amines is shown in Schemes 1-3. Three different classes of amines namely: two amino groups and a phenyl ring, two amino groups and aliphatic chain and one amino group and a phenyl ring were chosen so as to study the effect of the different substituents on the antimicrobial properties of the synthesized Schiff bases. The elemental analysis data of these compounds show that the amount of carbon, hydrogen and nitrogen are close to the experimentally determined values.

3.1 Electronic spectra

The ligand, 3,5-DA showed two absorption bands at 389 and 459 nm which were assigned $n-\delta^*$ and $n-\pi^*$ transition, respectively. The ligand, OAP showed an absorption band at 429 nm and TPMC/DDE also showed three absorption bands at 322, 314 and 310 nm that were assigned to $n-\pi^*$.

3.2 Infra red spectra

The strong IR absorption bands at 1618 cm^{-1} for 3,5-DA, 1637 cm^{-1} for OAP and 1598 cm^{-1} for TPMC/DDE were assigned to azomethine, C=N stretching vibrations. The strong bands at 1613 cm^{-1} for 3,5-DA, 1637 cm^{-1} for OAP and 1783 cm^{-1} , 1632 cm^{-1} for TPMC/DDE were assigned C=C stretching vibrations. Strong bands at 3122, 2981 cm^{-1} for 3,5-DA, 3117 cm^{-1} , 3003 cm^{-1} for OAP and 3182 cm^{-1} , 2852 cm^{-1} for TPMC/DDE were assigned C-H aromatic stretching vibrations. The broad bands at 3504 cm^{-1} for 3,5-DA and 3690 cm^{-1} for OAP were assigned OH stretching vibrations. The sharp strong band at 1942 cm^{-1} for 3,5-DA is assigned C=O of CO_2H .

3.3 1H NMR and ^{13}C NMR spectra

The 1H -NMR signal for the ligand, 3,5-DA at δ 9.60 (1H, d) was assigned to the aldimine proton of (H)C=N. The signals at δ 6.81-7.66 (7H, m) were



due to phenyl protons. The signals at δ 5.99 (1H, d), 6.03 (1H, d) correspond to ethylene protons. The signal at δ 6.33 (1H, s) was assigned to the carboxyl proton CO_2H . The signal at δ 2.16 (3H, s) is attributed to the methyl proton, OMe.

The ^1H NMR signal at δ 9.62 (1H, d) for the ligand, OAP was assigned to the aldimine proton, $(\text{H})\text{C}=\text{N}$. The signals at δ 6.82 (1H, t), 6.93 (1H, d) were attributed to ethylene protons $\text{HC}=\text{C}(\text{H})-\text{C}$. The signals at δ 6.98-7.59 (8H, m) were attributed to phenyl protons. The signal at δ 8.39 (1H, d) is assigned to the hydroxyl proton. The signal at δ 3.86 (3H, s) corresponds to the methyl protons, OMe.

The ^1H NMR signal of the ligand, TPMC/DDE at δ 6.69 (1H, d) was assigned to the aldimine proton $(\text{H})\text{C}=\text{N}$. The signals at δ 6.87 (1H, t), 6.98 (2H, d) were due to ethylene protons. The signals at δ 7.42 (2H, d), 7.94 (2H, d) were attributed to phenyl protons. The signal at δ 2.09 (3H, s) was assigned to the methyl protons, OMe.

The ^{13}C NMR signal for the ligand, 3,5-DA at 159.25 ppm was attributed to the azomethine $\text{C}=\text{N}$

carbon atom. The signal at 55.97 ppm was assigned to the methoxy, OMe carbon atom. The signals at δ 115.60-134.50 ppm correspond to the phenyl carbon atoms. The signal at 174.24 ppm was assigned to carboxylic acid carbon atom, CO_2H .

For the ligand, OAP the ^{13}C NMR signal at 162.64 ppm was attributed to azomethine carbon. The signal at 55.91 ppm is as a result of the OMe carbon atom. The signals at δ 115.49-157.88 ppm correspond to the phenyl carbon atoms. The signal at 161.79 ppm was due to methylene carbon atom.

For the ligand, TPMC/DDE the signal at 167.68 ppm was assigned to the azomethine $\text{C}=\text{N}$ carbon atom. The signal at 55.87 ppm was due to OMe carbon atom. The signals at δ 125.35-162.50 ppm were attributed to the phenyl carbon atoms. The signals at δ 60.89-71.62 ppm were assigned to the CH_2-CH_2 carbon atoms.

3.4 Antimicrobial Screening

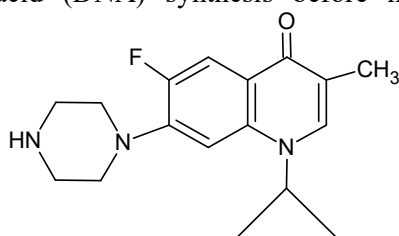
Table 1 shows the Inhibition Zone Diameter (IZD) and the Minimum Inhibition Concentrations (MIC) of the compounds.

Table 1: The Antimicrobial results of the compounds

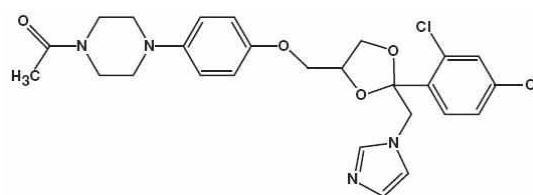
Sample	<i>Pseudomonas aeruginosa</i>		<i>Escherichia coli</i>		<i>Staphylococcus aureus</i>		<i>Bacillus subtilis</i>		<i>Aspergillus niger</i>		<i>Candida albicans</i>	
	IZD (mm)	MIC (mg/mL)	IZD (mm)	MIC (mg/mL)	IZD (mm)	MIC (mg/mL)	IZD (mm)	MIC (mg/mL)	IZD (mm)	MIC (mg/mL)	IZD (mm)	MIC (mg/mL)
3,5-DA	-	-	-	-	-	-	-	-	-	-	10.0	5.0
OAP	-	-	-	-	-	-	-	-	-	-	10.0	3.0
TPMC/DDE	8.0	7.5	10.0	1.9	-	-	-	-	-	-	15.0	1.6
Ciprofloxacin	5.0	6.0	10.0	1.1	2.0	2.0	10.0	2.3	-	-	-	-
Ketoconazole	-	-	-	-	-	-	-	-	15	3.2	11	1.3

Ciprofloxacin and ketoconazole were used as positive control while sterile DMSO served as negative control. The structures of these drugs are shown in Fig.1. Ciprofloxacin ($\text{C}_{17}\text{H}_{18}\text{FN}_3\text{O}_3$) belongs to fluoroquinolones and can inhibit bacteria growth by preventing deoxyribonucleic acid (DNA) synthesis before mitosis (Wolters,

2009). Ketoconazole ($\text{C}_{26}\text{H}_{28}\text{Cl}_2\text{N}_4\text{O}_4$) is a synthetic imidazole antifungal drug which can inhibit sterol 14- α -dimethylase, a microsomal cytochrome P450-dependent enzyme, thereby disrupting synthesis of ergosterol, an important component of the fungal cell wall (Kester *et al.*, 2012).



Ciprofloxacin



Ketoconazole

Fig. 1: Chemical structure of the drugs used as standard



Table 1 reveals that the ligands, 3,5-DA and OAP showed activity only against the fungus, *Candida albicans* with inhibition zone diameter (IZD) of 10mm and minimum inhibitory concentration of 5.0 mg/mL and 3.0 mg/mL respectively. TPMC/DDE gave the highest IZD of 15 mg/mL and MIC of 1.60 mg/mL against *Candida albicans*. The ligand, TPMC/DDE also showed varying activity against bacteria; *Pseudomonas aeruginosa* with an IZD of 8.0mm and MIC of 7.5 mg/mL; *Escherichia coli* with an IZD of 10.0mm and MIC of 1.9 mg/mL. The antibacterial activity of TPMC/DDE against *Escherichia coli* is comparable to that of Ciprofloxacin as shown in Table 1. Comparatively, the compounds showed close antifungal activity with the standard antifungal drug, ketoconazole. Therefore, the result showed that the compounds have good anti-fungal properties.

3.5 Molecular Simulation

The lipopolysaccharide layer around the cell wall of gram negative bacteria is one of the major features that differentiate them from their gram positive counterpart (Nwuche *et al.*, 2017). Antibiotic resistance has been attributed to the difficulty of passage of drugs across this layer (Nikaido, 1994). However, activities which tamper with the integrity of the bacteria cell wall could lead to death of the organism. One of the enzymes involved in the biosynthesis of bacteria cell wall is DD-transpeptidase (DDTP) (Poole, 2002). This makes the enzyme a choice drug target for the chemotherapy of bacterial infection. Moreover, it is not found in mammalian cells (Onoabedje *et al.*, 2016).

The grid box that defines the region of protein ligands search for possible binding interaction was

constructed to cover the entire macromolecules (DDTP and NMT) so as to recognize the possibility of binding at allosteric sites (potential binding sites other than the active site known inhibitors of the protein binds). Out of the three studied Schiff-bases only TPMC/DDE (free binding energy = -8.33 kcal/mol) dock into the known binding site groove of DDPT whereas 3,5-DA (free binding energy = -8.92 kcal/mol) and OAP (free binding energy = -8.58 kcal/mol) bind in allosteric sites and made interaction with residues different from those resident/surrounding the active site of the DDTP (Fig 2a). The best binding conformation of the ligands in DDPT active cavity as retrieved from the lowest theoretical binding free energy suggests that 3,5-DA and OAP inhibit the activity of DDPT and hence better antibiotic molecules than TPMC/DDE. However, the contrary antibiotic *in vitro* screening infers that either the binding of 3,5-DA and OAP at the allosteric sites are not stable enough within the physiological time necessary to initiate pharmacological effect or the conformational change(s) undergone by the protein consequence of the presence of the ligands at the allosteric site could not prevent DDPT catalytic activity. The flexibility of the TPMC/DDE enabled it to fold into the binding cavity of the protein as other known inhibitors of DDTP (-8.33 kcal/mol). Binding interaction between it and DDTP was mainly characterized by π - π bonding occurring between the phenyl rings of the compound and the aromatic groups of Phe120, Tyr157, Tyr 159, and Tyr 306 (Fig 2a). In addition, methoxyl and NH groups of the ligand were found to be involved in H-bonding with Arg285, Thr299 and Asn161.

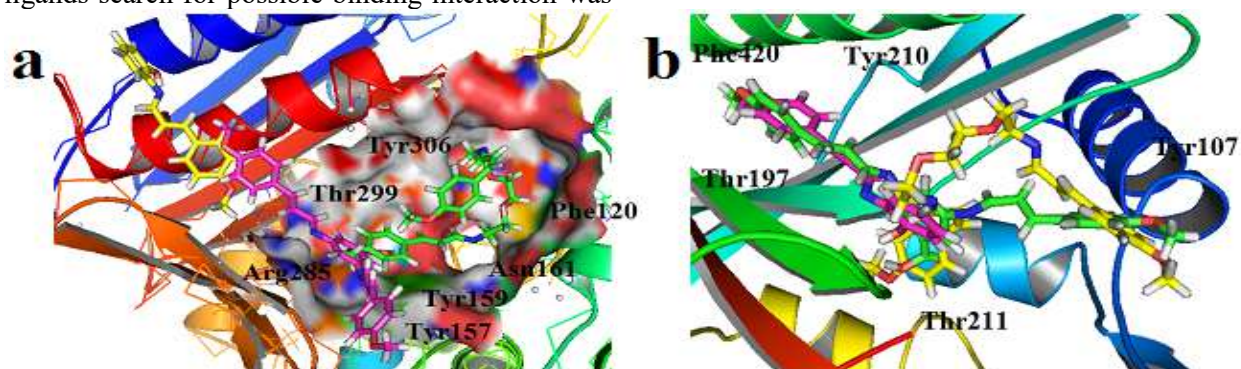


Fig. 2: Binding poses of 3,5-DA, OAP and TPMC/DDE toward DDTP and NMT. The carbon atoms in 3,5-DA, OAP and TPMC/DDE are coloured in green, purple and yellow, respectively while other atoms retain their standard colours.



NMT is a pre-clinically validated protein targeted for the treatment of fungal infections. NMT functions as a catalyst for the attachment of the fatty acid and myristate to protein substrate (N-myristoylation) (Bell *et al.*, 2012; Sogabe *et al.*, 2002). The best dock poses of the ligands (3,5-DA = -12.99 kcal/mol, OAP = -11.24 kcal/mol and TMPC/DDE = -11.75 kcal/mol)(Fig. 2b) toward NMT binding site showed that the ligand interacted (π - π bonding) with the protein Tyr157, Tyr159, Tyr306 and Phe120 phenyl rings through their terminal aromatic groups. It was also observed that the ligands used their carboxylate, hydroxyl and methoxyl groups respectively, to H-bond with NMT Thr211. The calculated binding affinity derived from docking studies validates the *in vitro* antifungal potencies of the Schiff-bases.

4.0 Conclusion

The syntheses of the Schiff bases, 3,5-bis[(E)-[(2E)-3-(4-methoxyphenyl)prop-2-en-1-ylidene]benzoic acid, 2-[(E)-[(2E)-3-(4-methoxyphenyl)prop-2-en-1-ylidene]amino]phenol and [3-(4-methoxyphenyl)-allylidene]-[2-(2-{2-[3-(4-methoxyphenyl)-allylideneamino]-ethoxy}-ethoxy)-ethyl]-amine were achieved successfully. The Schiff bases were characterized using UV-visible, infrared, ^1H and ^{13}C NMR spectroscopy. The antimicrobial activities of the compounds were compared with those of ciprofloxacin as standard antibacterial drug and ketoconazole as anti-fungal drug. The antimicrobial screening shows that the ligands are promising fungicidal agent. The molecular docking results justified the observed *in vitro* antimicrobial properties of the ligands. Moreover, the compound, TMPC/DDE, emerged as the most promising antibiotic and antifungal candidate and is worth receiving further attention to develop it into a new and better antimicrobial agent.

5.0 Acknowledgements

Prof. Klaus Jurkschat of Technische Universität, Fakultät für Chemie und Chemische Biologie, D-44221 Dortmund, Germany is acknowledged for helping with the spectral analyses. Dr. Ibezim Akachukwu is grateful to AGNES (African-German Network of Excellence in Sciences) for the award of Junior Researchers Grant (JRG) and Dr. Ntie-Kang Fidele for providing computational resources.

6.0 References

Ahamad, R. P. & Quaraiishi, M. A.(2010). Thermodynamic, electrochemical and quantum

chemical investigation of some Schiff bases as corrosion inhibitors for mild steel in hydrochloric acid solutions. *Corrosion Science*, 52(3), pp. 933-942.

Andrew, S., Clayton, H. H. & Edward, M. K.(1992). *Introduction to Organic Chemistry*, 4th Edition, Macmillan Publishing Company, USA, pp. 399.

Arun, S., Bhupendra J., Ruchi D. (2002). Process for the preparation of substituted trans-cinnamaldehyde, a natural yellow dye, from phenylpropane derivatives. *US20020133045A1*.

.Bansode, V. J. (2012). A review on Pharmacological activities of cinnamionium cassia Blume. *International Journal of Green Pharmacy*, 6, pp. 102-108.

Bell, A. S., Mills, J. E., Williams, G. P., Brannigan, J. A., Wilkinson, A. J., Parkinson, T., Leatherbarrow, R. J., Tate, E. W., Holder, A. A., Smith, D. F. (2012). Selective inhibitors of protozoan protein N-myristoyltransferases as starting points for tropical disease medicinal chemistry programs. *PLoS Neglected Tropical Diseases*, 6(4):e1625, DOI: 10.1371/journal.pntd.0001625.

Berman, H. M., Westbrook, J., Feng, Z., Gilliland, G., Bhat, T. N., Weissig, H., Shindyalov, I. N., Bourne, P. E. (2000). The protein data bank. *Nucleic Acids Research*, 28, pp. 235-342.

Chah, K. F., Eze, C. A., Emuelosi, C. E. & Esimone, C. O. (2006). Antibacterial and Wound Healing properties of Methanolic Extracts of some Nigerian Medicinal plants. *Journal of Ethnopharmacology* 104, 164, pp. 164 – 167.

Finar, I. L. (2006). *Organic Chemistry*, 5th Edition, Darling Kindersley Publishing Co. India, pp. 844-847.

Golcu, A., Tumer, M., Demirelli, H. & Wheatley, R. A. (2005). Cd(II) and Cu(II) complexes of polydentate Schiff base ligand: synthesis, characterization, properties and biological activity. *Inorganica Chimica Acta*, 358, pp. 1785-1795.

Halgren, T. A. (1996). Merck molecular force field. *Journal of Computational Chemistry*, 17, pp. 490-641.

Iihan, S., Temel, H., Yilmaz, J. & Sekera, M. (2007). Synthesis, structural characterization and electrochemical studies of New macrocyclic Schiff base containing pyridine head and its



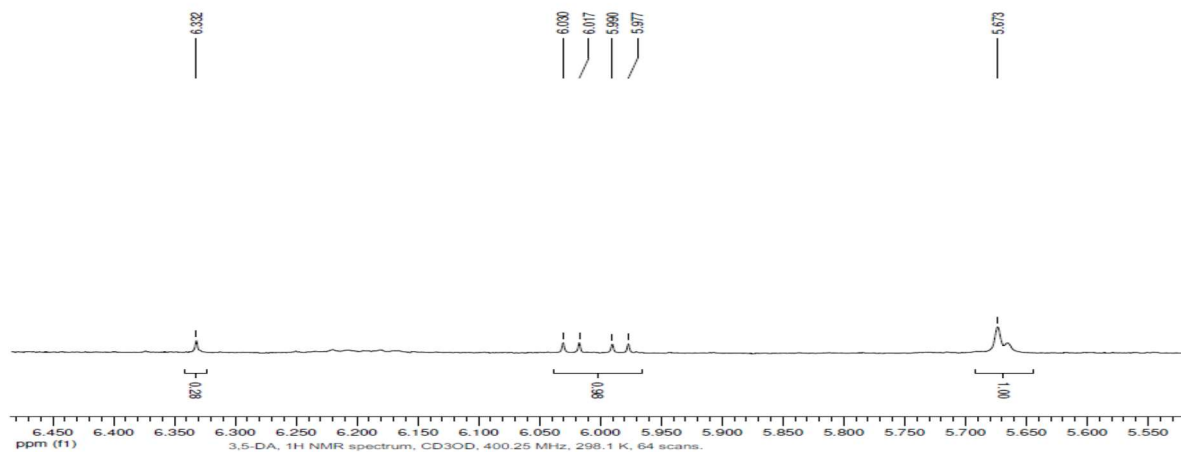
- metal complexes. *Journal of OrganoChemical Chemistry*, 6, 9, pp. 3855-3865.
- Ikechukwu, P. E. & Peter, A. A. (2015). Synthesis, Characterization and Biological Studies of metal (II) Complexes of (3E-3-(2-{E)-(1-[2, 4-Dihydroxyphenylethylidene]amino}ethyl)imino]-1-phenylbutan-1-one Schiff Base. *Molecules*, 20, pp. 9788-9802.
- Keshvari, M., Asgary, S., Jafarian-Dehkordi, A., Najafi, S., & Ghoreyshi-Yazdi, S. M. (2013). Preventive effect of cinnamon essential oil on lipid oxidation of vegetable oil, *ARYA Atherosclerosis*, 9, 5, pp. 280-286.
- Kester, M., Karpa, K. D. & Vrana, K. E. (2012). Elsevier's Integrated Review Pharmacology (Second Edition, pp. 41-78.
- Kong, J.-O., Lee, S.-M., Moon, Y.-S., Lee, S.-G. & Ahn, Y.-J. (2007). Nematicidal Activity of Cassia and Cinnamon Oil Compounds and Related Compounds toward *Bursaphelenchus xylophilus* (Nematoda: Parasitaphelenchidae). *Journal of Nematology*, 39, 1, pp.31-36.
- Mangaiyarkkara, S. P. & Aru, A. S. (2014). Synthesis, Spectral Characterization and Antimicrobial Studies of Some Novel Schiff, Base Metal Complexes of Vanilin, based Dihydropyrimidone Heterocyclic Product and 4-Aminoantipyrine. *Asian Journal of Science and Technology*, 5, 6, pp. 340-347.
- Mashaly, M. M., Abd-Elwahab, Z. & Faheim, A. A. (2004). Preparation, Spectral, Characterisation and Antimicrobial activities of Schiff base complexes derived from 4-aminoantipyrine, mixed ligand complexes with 2-Aminopyridine 8-hydroxyquinoline and oxalic acid and their pyrolytic products. *Journal of Chinese Chemical Society*, 5, 5A, pp. 901-915.
- Mohammed, N. I & Salaheddin, A. I. S. (2011). Synthesis, characterization and uses of Schiff base as fluorimetric analytical reagents. *E-Journal of chemistry*, 8, 1, pp. 180-184.
- Molecular Operating Environment, version 2010; Chemical Computing Group Inc: Montreal, Canada, 2010.
- Mokhles, M. A., Mohammad, M. E., Shakodofa, H. A. & Samia, A. M. (2014). Synthesis, characterization and biological activity of some Ferrocenyl complexes containing Antipyrine Moiety. *Transactions on Applied Chemistry*, 1, 1, pp. 42-52.
- Mostafa, M. H. K., Eman, H. I., Gehad, G.M., Eheeb, M. Z. & Ahmed, B. (2012). Synthesis and characterization of a novel schiff base metal complexes and their application in determination of iron in different types of natural water. *Open Journal of Inorganic Chemistry*, 2, 2, pp. 13-21.
- Nikaido, H. (1994). Prevention of drug access to bacterial targets: permeability barriers and active efflux. *Science* 264:382±388 PMID: 8153625
- Nwuche, C. O., Ujam, O. T., Ibezim, A., & Ujam, I. B. (2017). Experimental and In-Silico Investigation of Anti-Microbial Activity of 1-Chloro-2-Isocyanatoethane Derivatives of Thiomorpholine, Piperazine and Morpholine. *PLoS ONE* 12(1):e0170150. doi:10.1371/journal.pone.0170150
- Obasi, N. L., Kaior, G. U., Ibezim, A., Ochonogor, A. E., Rhyman, L., Uahengo, V., Lutter, M., Jurkschat, K., & Ramasami, P. (2017). Synthesis, characterization, antimicrobial screening and in silico studies of Schiff bases derived from trans-paramethoxycinnamaldehyde. *Journal of Molecular structure*, 1149, pp. 8-16.
- Obasi, N. L., Kaior, G. U., Rhyman, L., Ibrahim, A. A., Hoong-Kun, F., & Ramasami, P. (2016) Synthesis, Characterization, Antimicrobial Screening and Computational Studies of 4[-3-(4-methoxy-phenyl)-allylideneamino]-1,5-dimethyl-2-phenyl-1,2-dihydro-pyrazol-3-one. *Journal of Molecular Structure* 1120, pp. 180-186.
- Ojo, O. O., Ajayi, A. O. & Anibjuwon, I. I. (2007). Antibacterial potency of Extract of lower plants, *Journal of Zhejiang University Sciences*, 8 (3), pp. 189- 191.
- Onoabedje, E. A., Ibezim, A., Okafor, S. N., Onoabedje, U. S., & Okoro, U. C. (2016). Oxazin-5-Ones as a Novel Class of Penicillin Binding Protein Inhibitors: Design, Synthesis and Structure Activity Relationship. *PLoS ONE* 11, 10, e0163467. doi:10.1371/journal.pone. 0163 4 67
- Ooi, L. S.M., Li, Y., Kam, S. -L., Wang, H., Wong, E. Y. L., & Ooi, V. E. C. (2006). Antimicrobial Activities of Cinnamon Oil and Cinnamaldehyde from the Chinese Medicinal Herb *Cinnamomum cassia* Blume. *American Journal of Chinese Medicine*, 34,3, pp. 511-522.



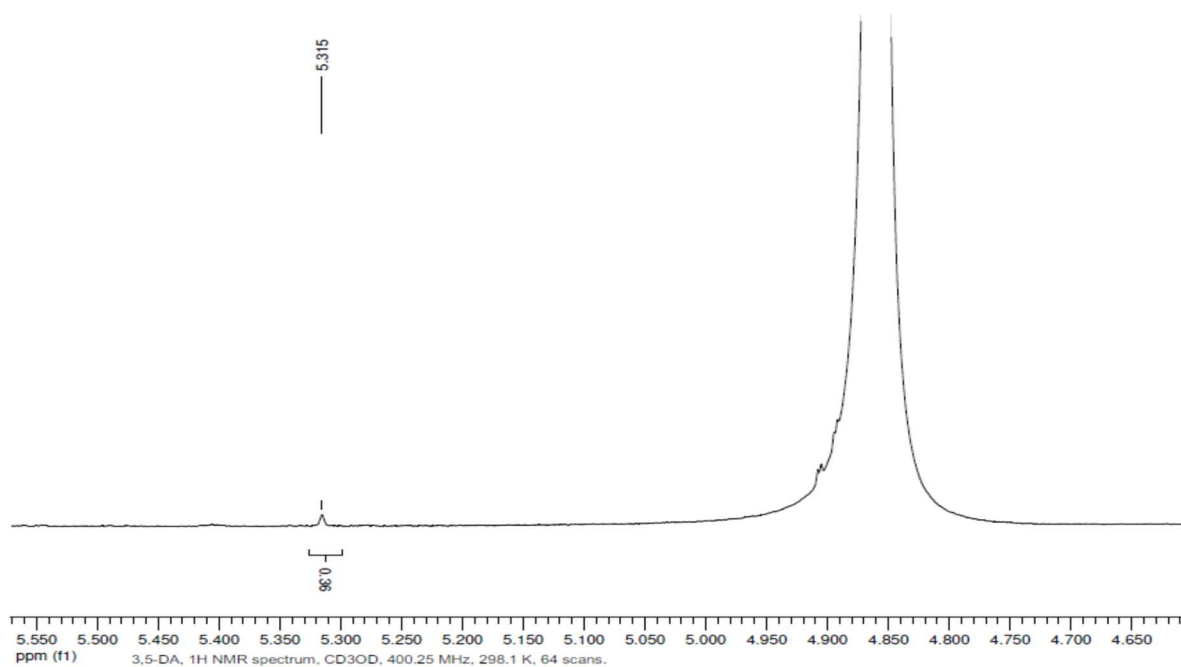
- Pallavi, G., Dinesh, K. & Sulekh, C. (2014). Schiff Base ligands and their transition metal complexes as Antimicrobial Agents. *Journal of Chemical Biological and Physical Sciences*, 4, 3, pp. 1946-1964.
- Poole, K. (2002). Mechanisms of bacterial biocide and antibiotic resistance. *Journal of Applied Microbiology*, Symposium Supplement, 91, pp.55-64.
- Prakash, A. & Adhikari, D. (2011). Application of Schiff bases and their metal complexes-A Review. *International Journal of Chemical Technology Research*, 3, 4, pp. 1891-1896.
- Raman, N., Ravichandran, S. & Thangaraja, C.(2004).Copper (II), cobalt(II), nickel(II), zinc(II) complexes of Schiff base derived from Benzil -2,4- dinitrophenylhydrazone with Aniline. *Journal of chemical sciences*, 116, 4, pp. 215-219.
- Rhohini, C. & Arul, A. S. (2014). Synthesis and Characterization of Bio-inorganic Transition Metal Complexes Derived From Novel Bignelli Adduct Coupled Schiff Bases. *International Journal of Pharmaceutical Sciences and Research*, 2, 10, pp. 4339-4350.
- Schmid, G. H. (1996). *Organic Chemistry Mossby Year Book*, 5th Edition, St Lious Missouri, pp. 620-628
- Seelolla, G., Cheera, P., & Ponneri, V. (2014). Synthesis, Antimicrobial and Antioxidant Activities of Novel series of Cinnamamide Derivatives having Morpholine Moiety. *Medicinal chemistry*, 4, pp. 778-783.
- Sobola, A. O., Watkins, G. M. & Brecht, B. V. (2014). Synthesis, characterization and antimicrobial activity of copper (II) complexes of some ortho-substituted aniline Schiff bases; crystal structure of bis(2-methoxy-6-imino)methylphenol copper(II) complex. *South African Journal of Chemistry*, 67, pp. 45-51 .
- Sogabe, S., Masubuchi, M., Sakata, K., Fukam, T. A., Morikami, K., Shiratori, Y., Ebiike, H., Kawasaki, K., Aoki, Y., Shimma, N., D'Arcy, A., Winkler, F. K., Banner, D. W. & Ohtsuka, T.(2002). Crystal Structures of *Candida albicans* N-Myristoyltransferase with Two Distinct Inhibitors. *Chemistry & Biology*, 9(10), pp. 1119-1128.
- Suresh, M. S. & Prakash, V. (2011). Preparation, characterisation and Antibacterial Studies of Chelates of Schiff Base Derived from 4-aminoantipyrine, furfural and O-phenylamine. *E- Journal of Chemistry*, 8, 3, pp. 1408-1416.
- Thomas, M., Kulandaisamy, A. & Manohar, A. (2012). Synthesis, spectral characterization, Redox and biological screening studies of Schiff base transition metal complexes. *Journal of Pharmacy Research*, 5, 1, pp. 86-90
- Vogel, A. I. (1989). *Vogel's Textbook of practical Organic Chemistry*, 5th Edition, Longman Scientific and Technical, Longman House, Burnt Mill, England, pp. 782, 900, 1412-1435.
- Wang, K. C., Chang, J. S., Chiang, L. C. & Lin, C. C. (2009). "4-Methoxycinnamaldehyde inhibited human respiratory syncytial virus in a human larynx carcinoma cell line". *Phytomedicine*. 16, 9, 882–886.
- Wolters, K. (2009). *Clinical Pharmacology made Incredibly Easy*, 3rd ed.; Lippincott, W and Wilkins: USA, pp. 256, 257.
- Yannai, S. (2004). *Dictionary of food compounds with CD-ROM: Additives, flavors, and ingredients.*, Chapman & Hall/CRC, Boca Raton, xvii, pp. 1763.
- Yuan, H., Wang, H., Li, Z., Li, S., Zhang, Y. & Chen, Y. (2015). Synthesis and antifungal property of N,N'-bis(trans-cinnamaldehyde)-1,2-diiminoethane and its derivatives. *Journal of Toxicological & Environmental Chemistry*, 2015, 97, 3-4, pp. 429-438.

7.0 Appendices



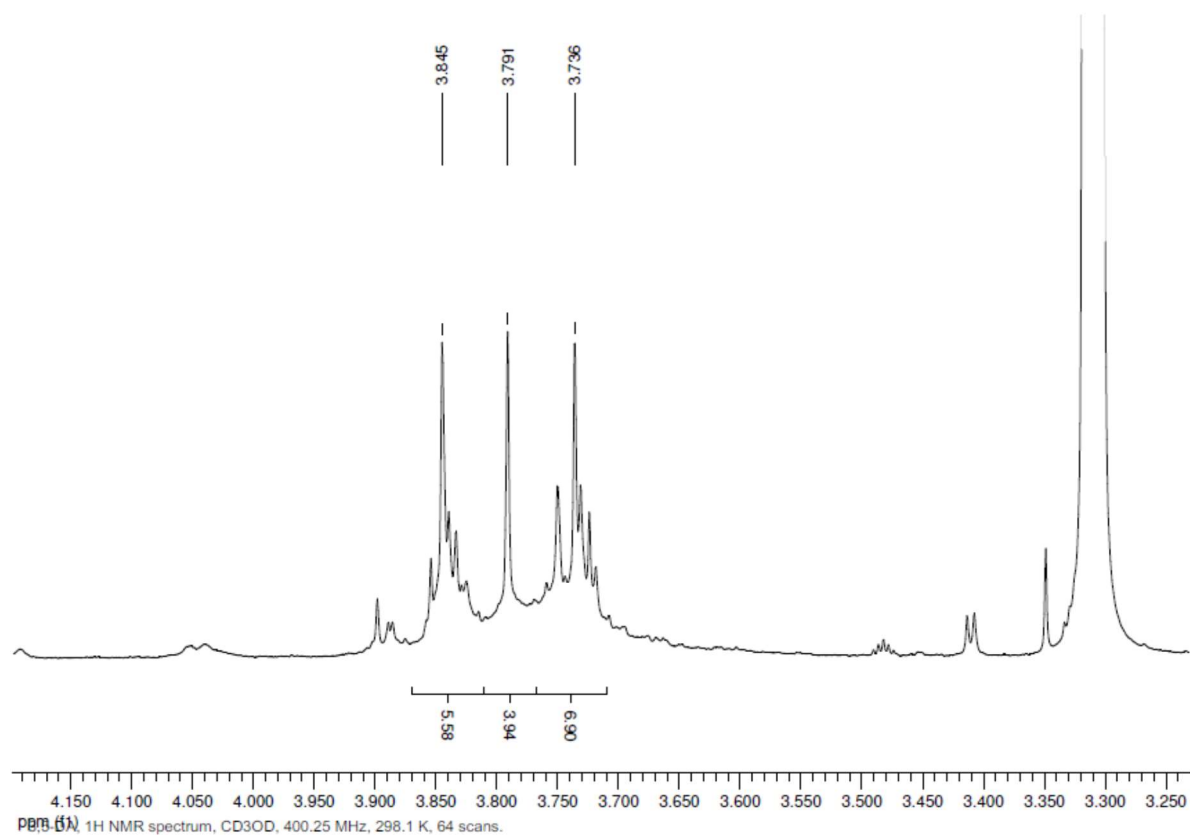


Appendix1(c): Experimental ^1H NMR Spectra of 3,5 DA showing peaks 5.675 – 6.332

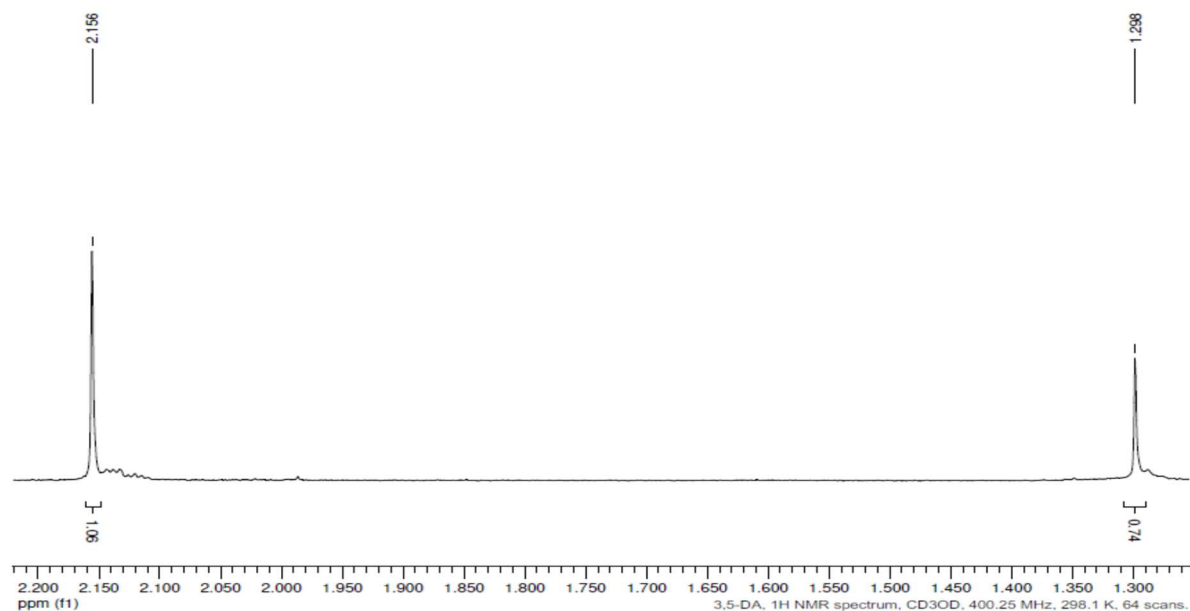


Appendix1 (d): Experimental ^1H NMR Spectra of 3,5 DA showing peaks at 5.315ppm



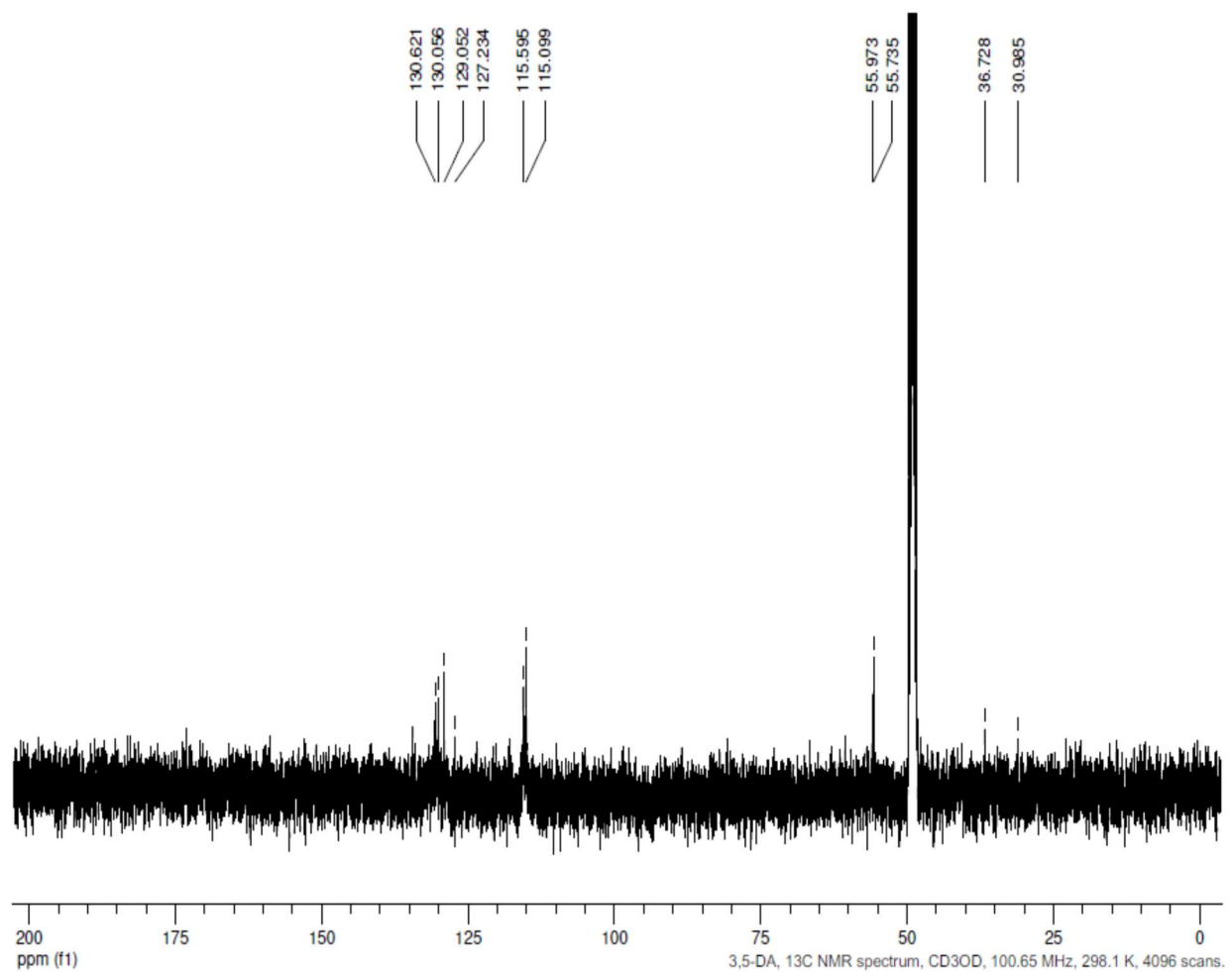


Appendix1 (e): Experimental ¹H NMR Spectra of 3,5 DA showing peaks 3.736 – 3.845 ppm



Appendix1 (f): Experimental ¹H NMR Spectra of 3,5 DA showing peaks 1.298 and 2.156 ppm

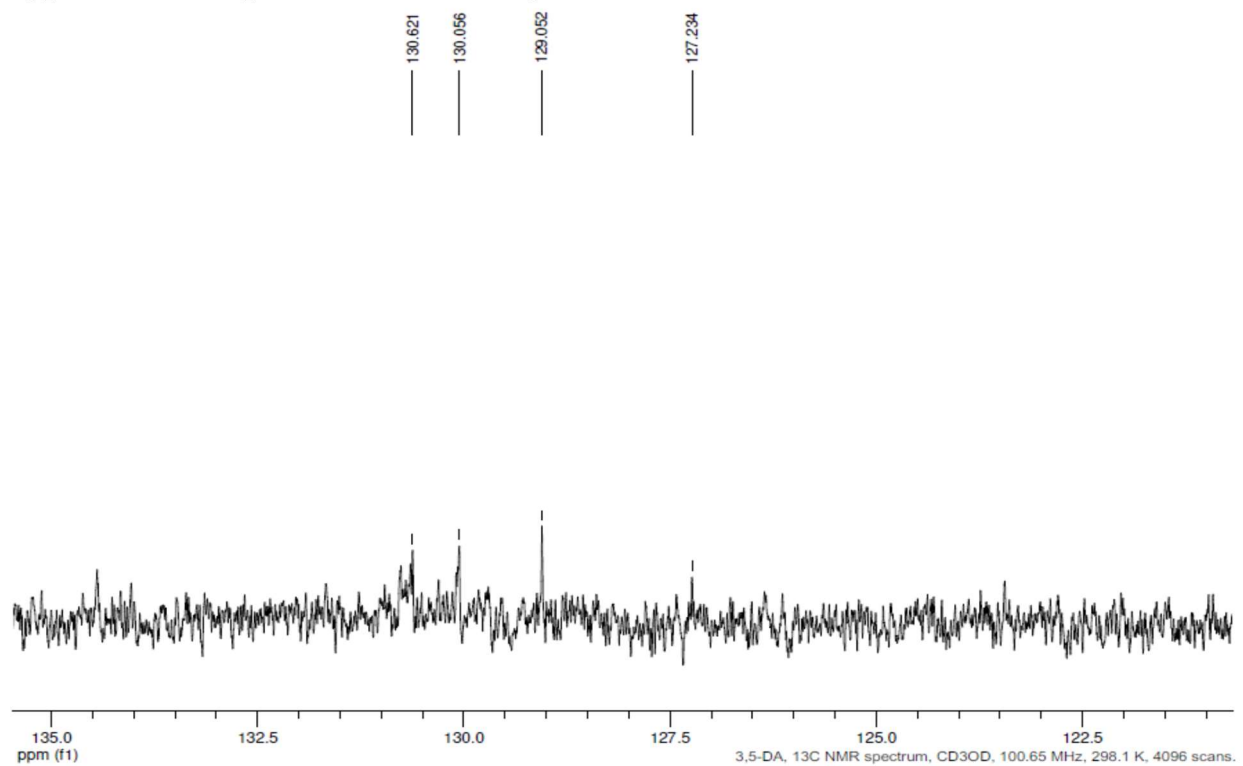




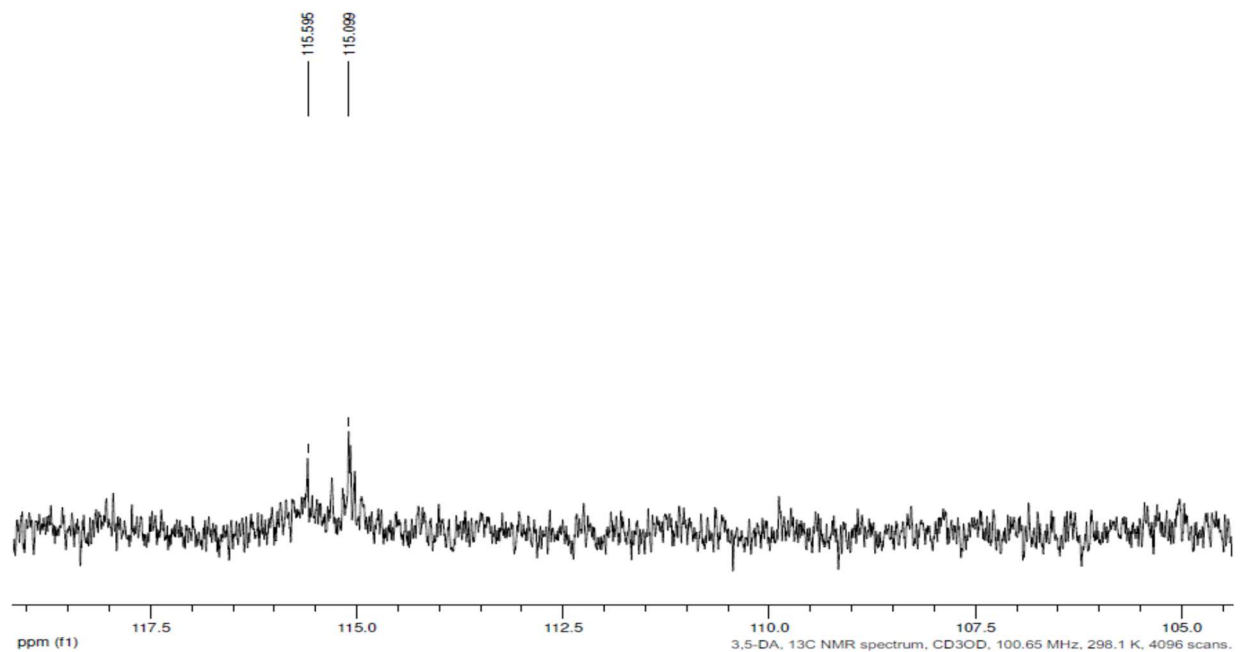
Appendix 2: Experimental ¹³C NMR Spectra of 3,5 DA



Appendix 2 (a): Experimental ^{13}C NMR Spectra of

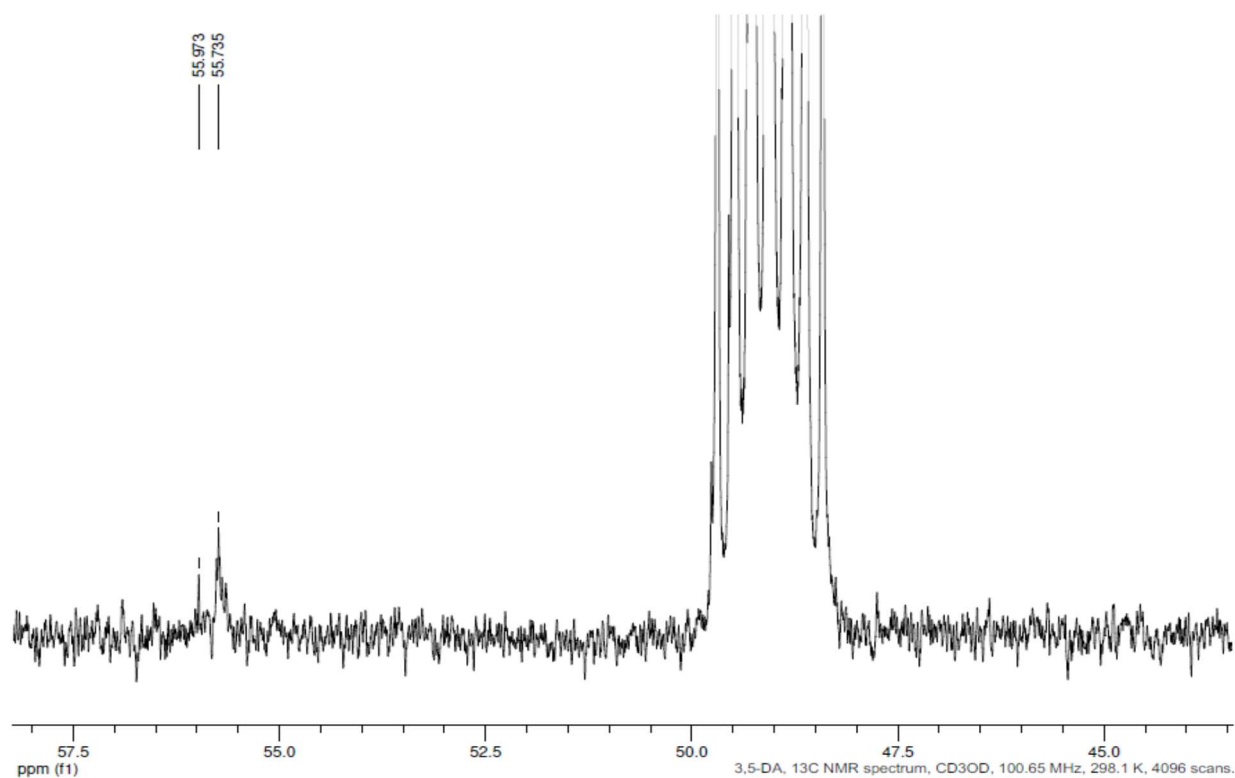


3,5 DA showing peaks 127.234 – 130.621ppm

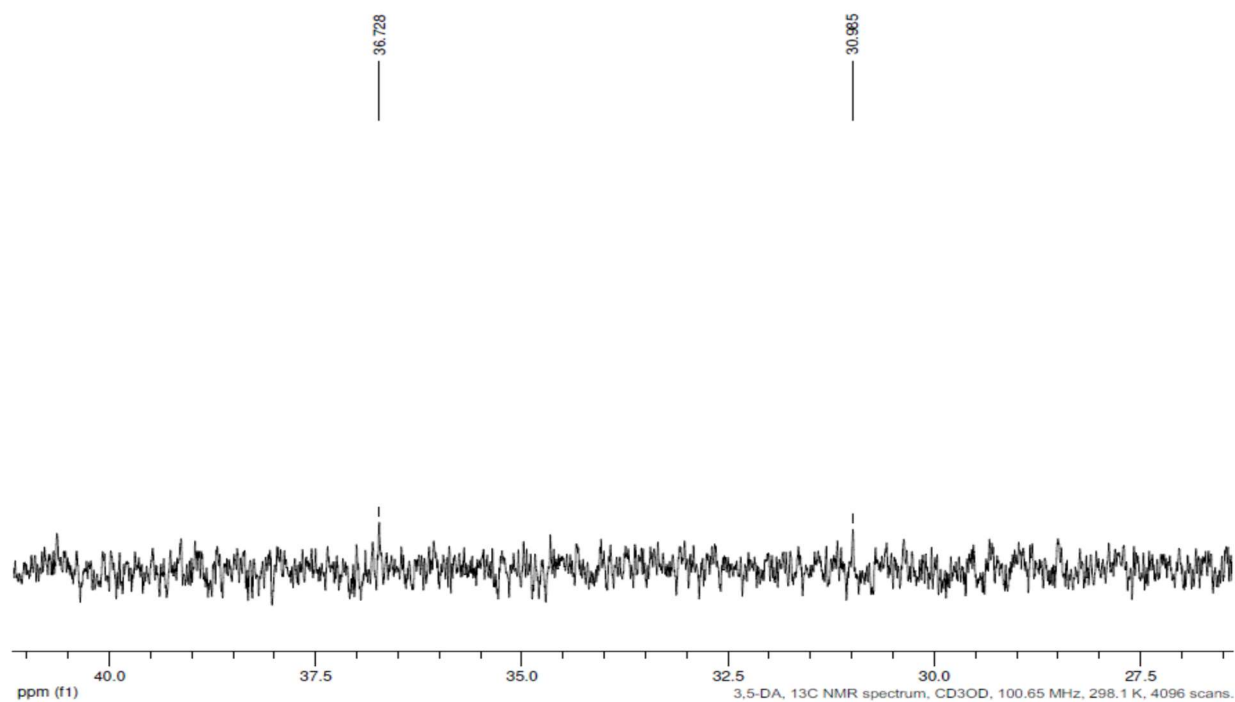


Appendix 2 (b): Experimental ^{13}C NMR Spectra of 3,5 DA showing peaks 115.099 – 115.595ppm



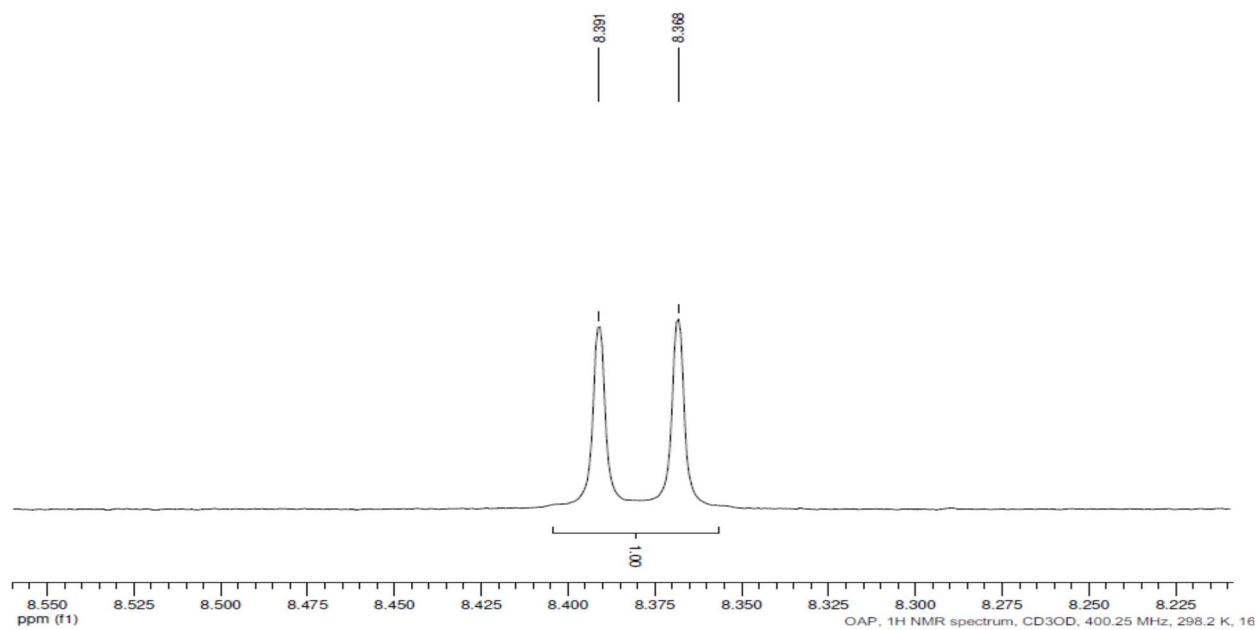


Appendix 2(c): Experimental ¹³C NMR Spectra of 3,5 DA showing peaks 55.735 and 55.973 ppm

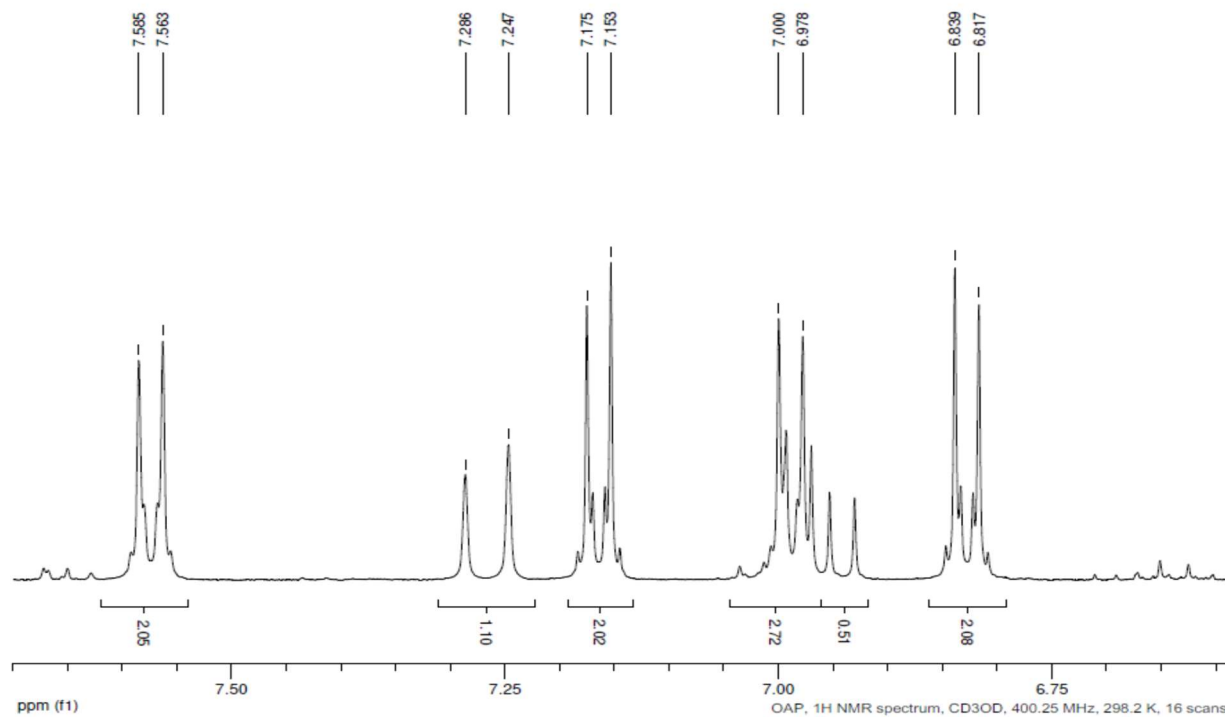


Appendix 2 (d): Experimental ¹³C NMR Spectra of 3,5 DA showing peaks 30.985 and 36.728 ppm



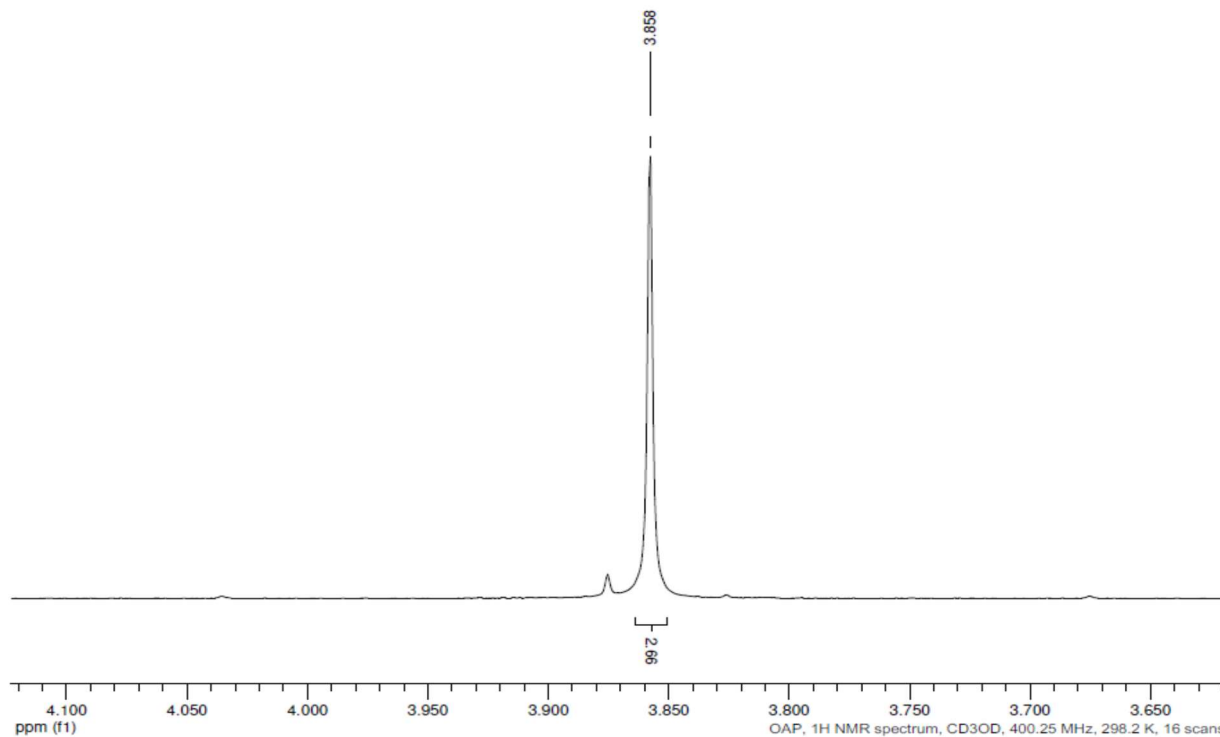


Appendix 3 (b): Experimental ¹H NMR Spectra of OAP showing peaks 8.368 and 8.391

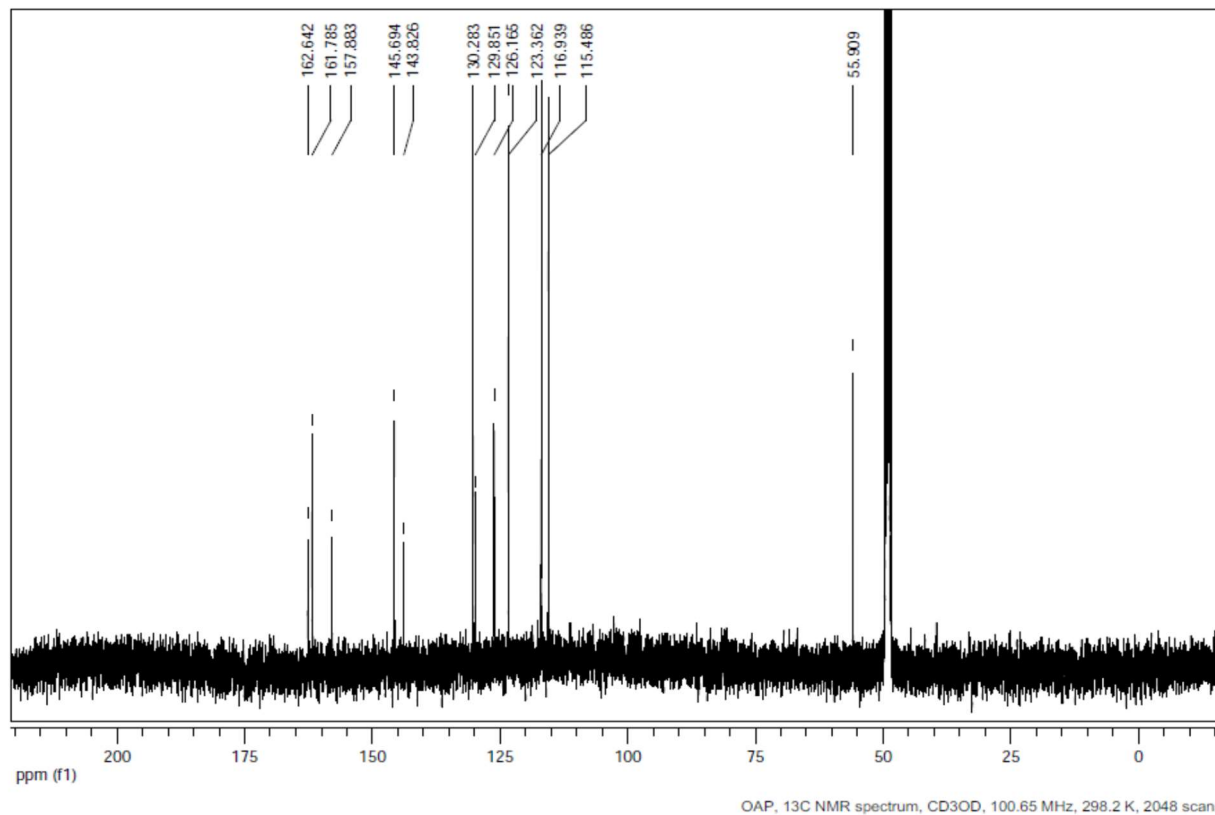


Appendix 3(c): Experimental ¹H NMR Spectra of OAP showing peaks 6.817- 7.585 ppm



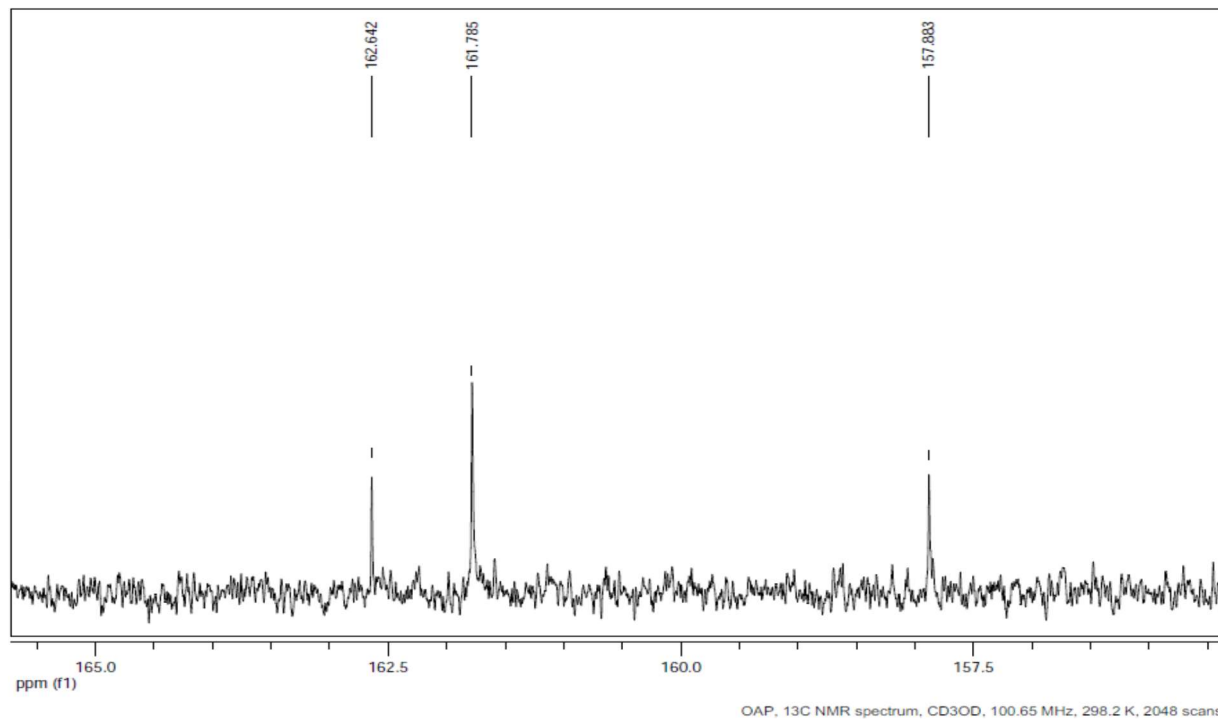


Appendix 3 (d): Experimental ¹H NMR Spectra of OAP showing peak 3.858 ppm

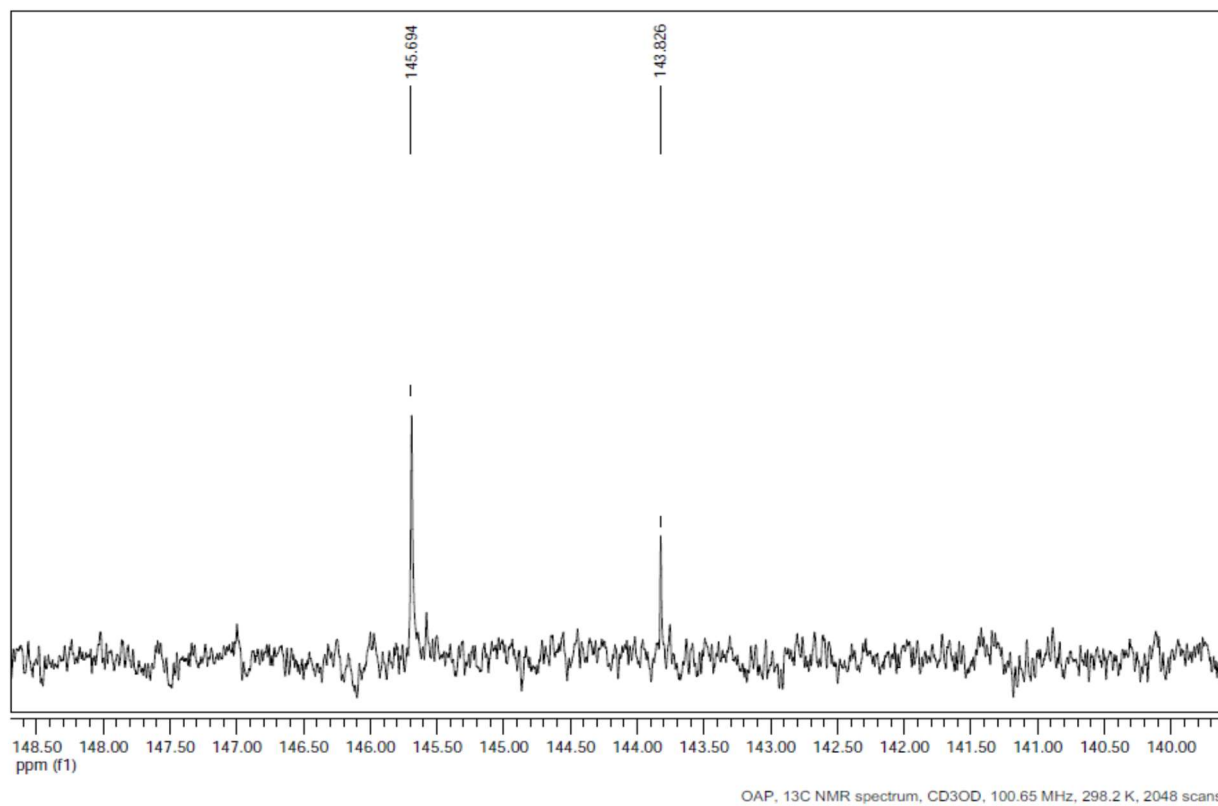


Appendix 4: Experimental ¹³C NMR Spectra of OAP



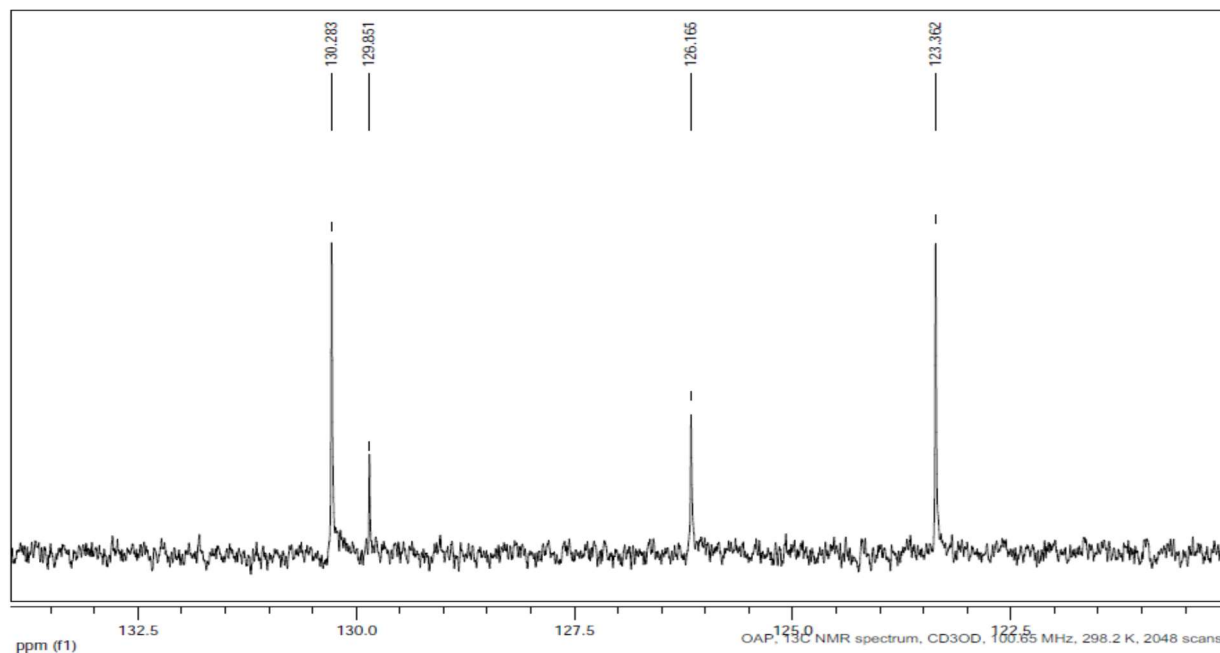


Appendix 4 (a): Experimental ¹³C NMR Spectra of OAP showing peaks 157.883 – 162.642 ppm

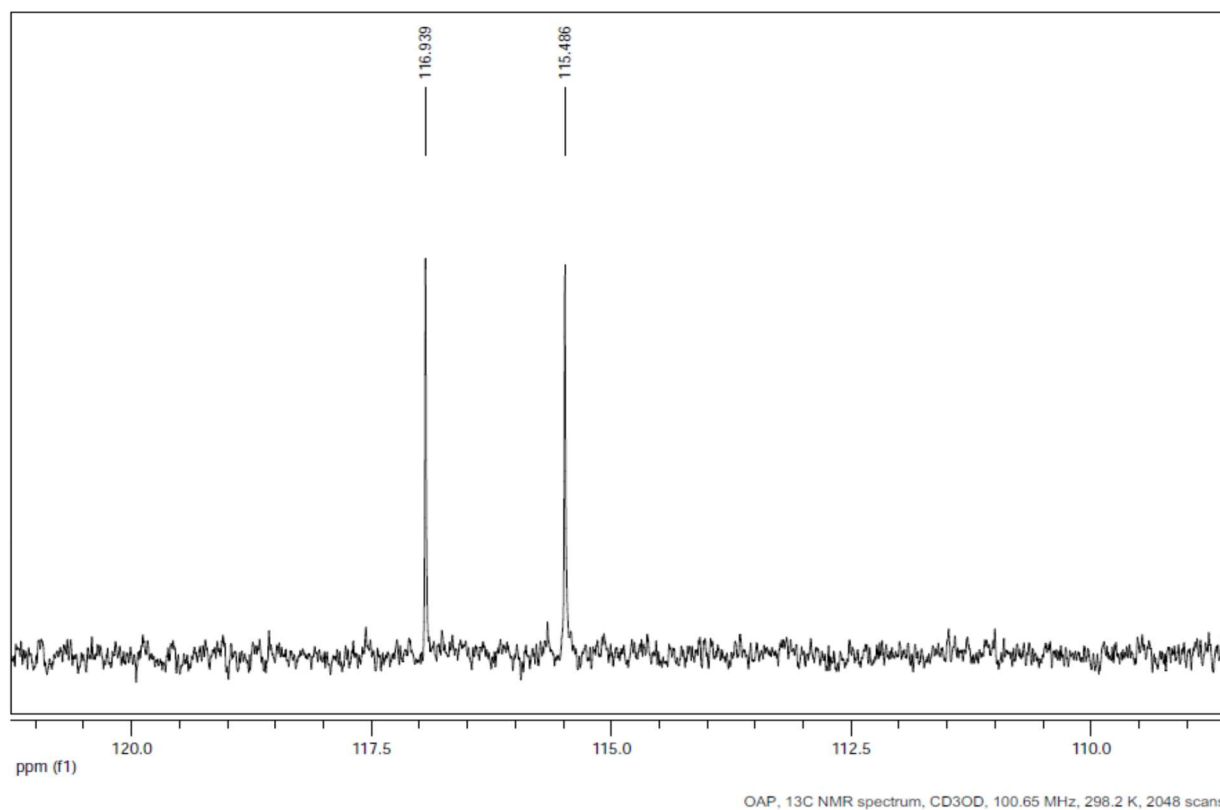


Appendix 4 (b): Experimental ¹³C NMR Spectra of OAP showing peaks 143.826 and 145.694 ppm



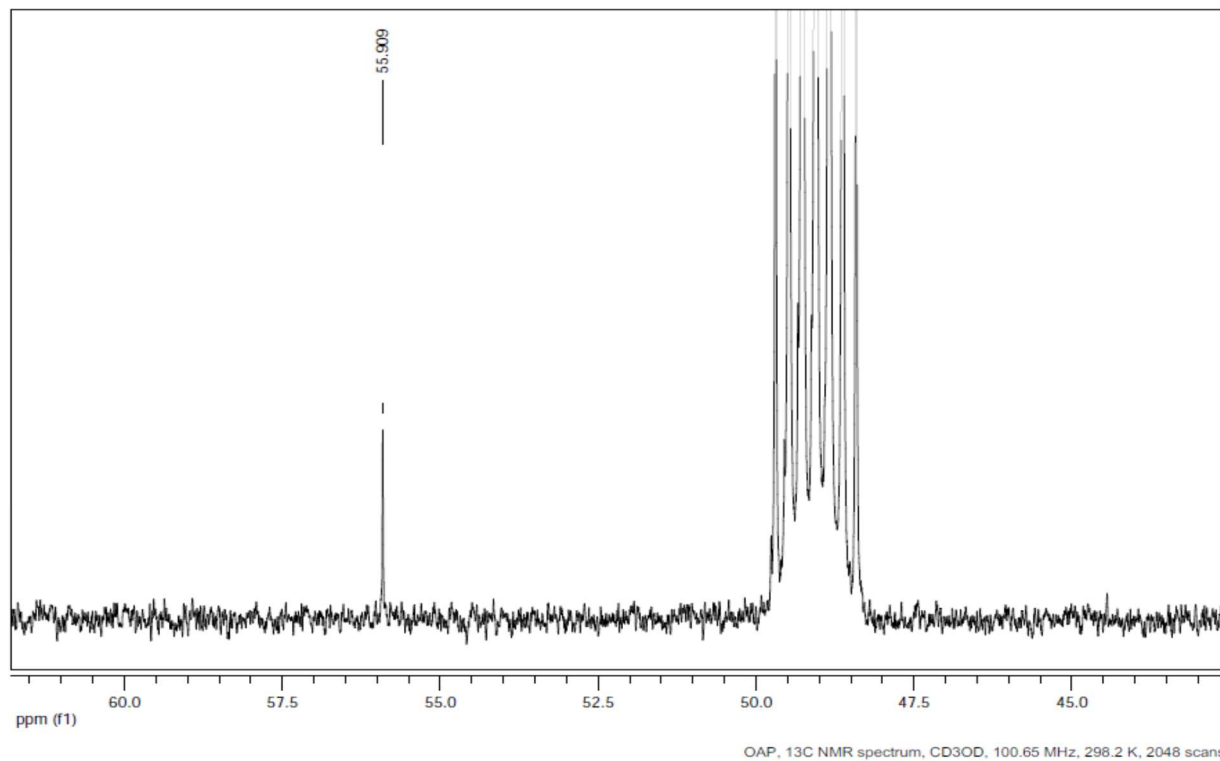


Appendix 4 (c): Experimental ¹³C NMR Spectra of OAP showing peaks 123.632 – 130.283 ppm

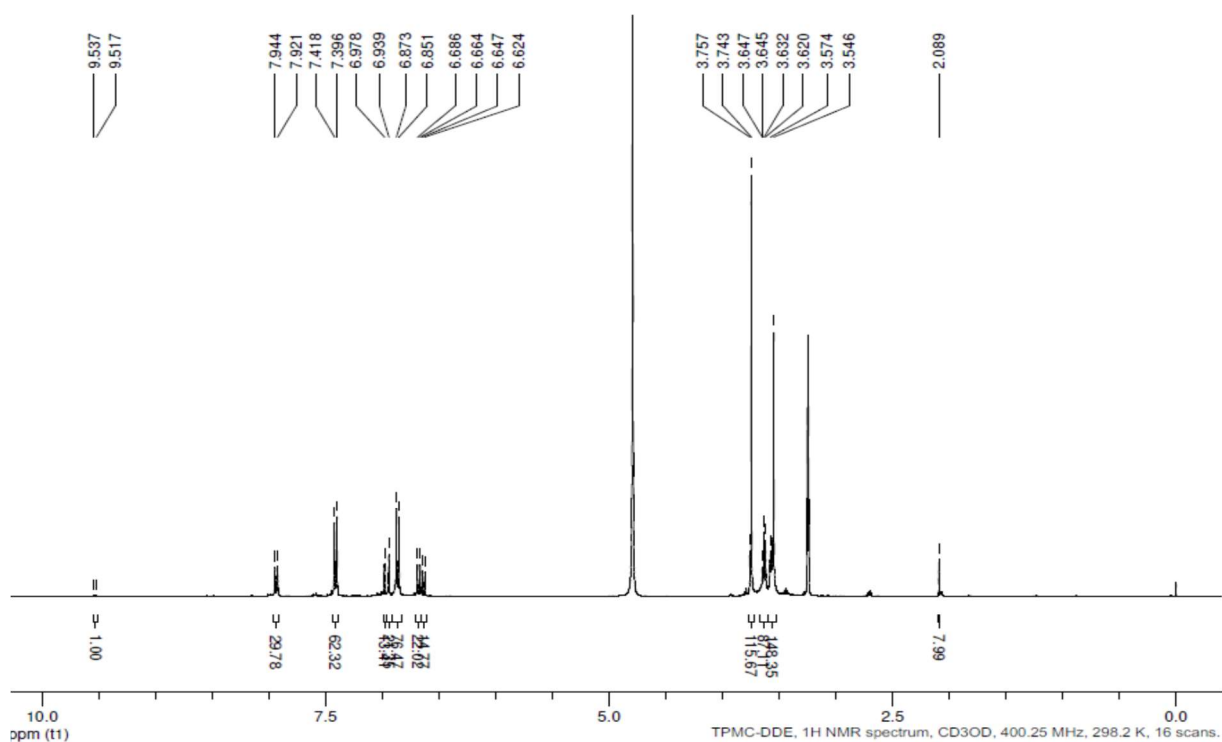


Appendix 4 (d): Experimental ¹³C NMR Spectra of OAP showing peaks 115.486 – 116.939 ppm



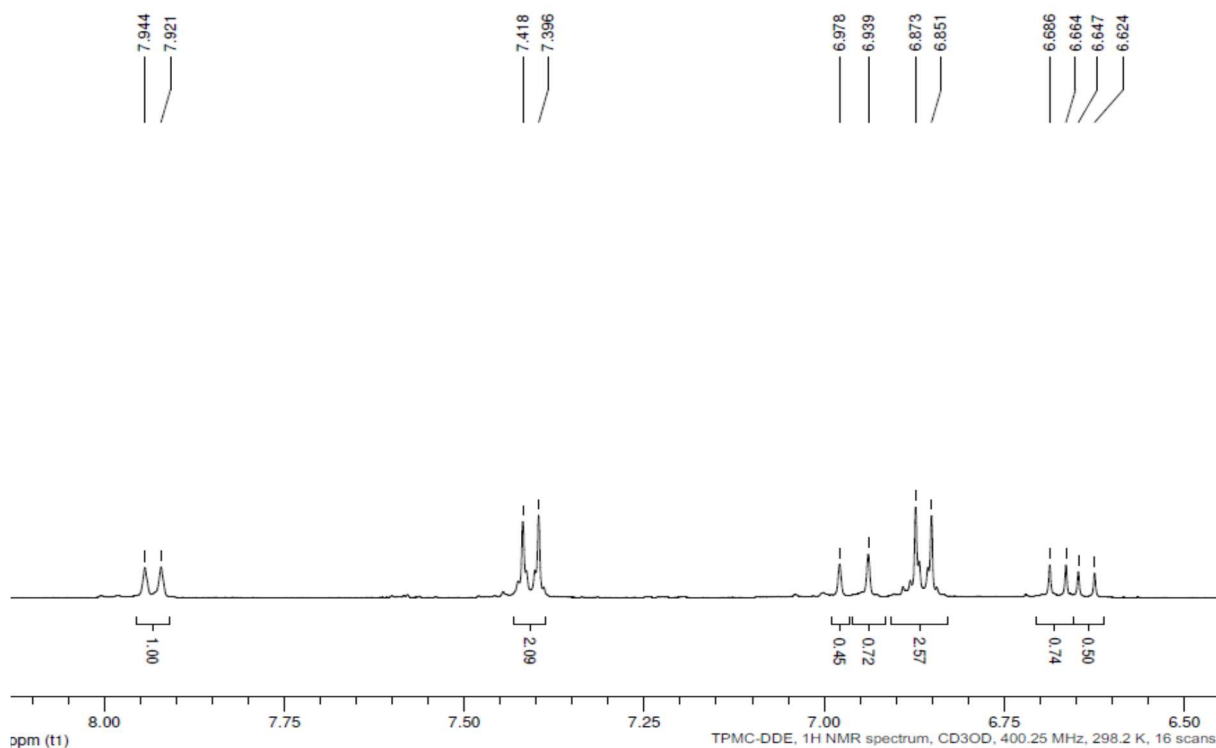


Appendix 4 (e): Experimental ¹³C NMR Spectra of OAP showing peaks 55.909 ppm

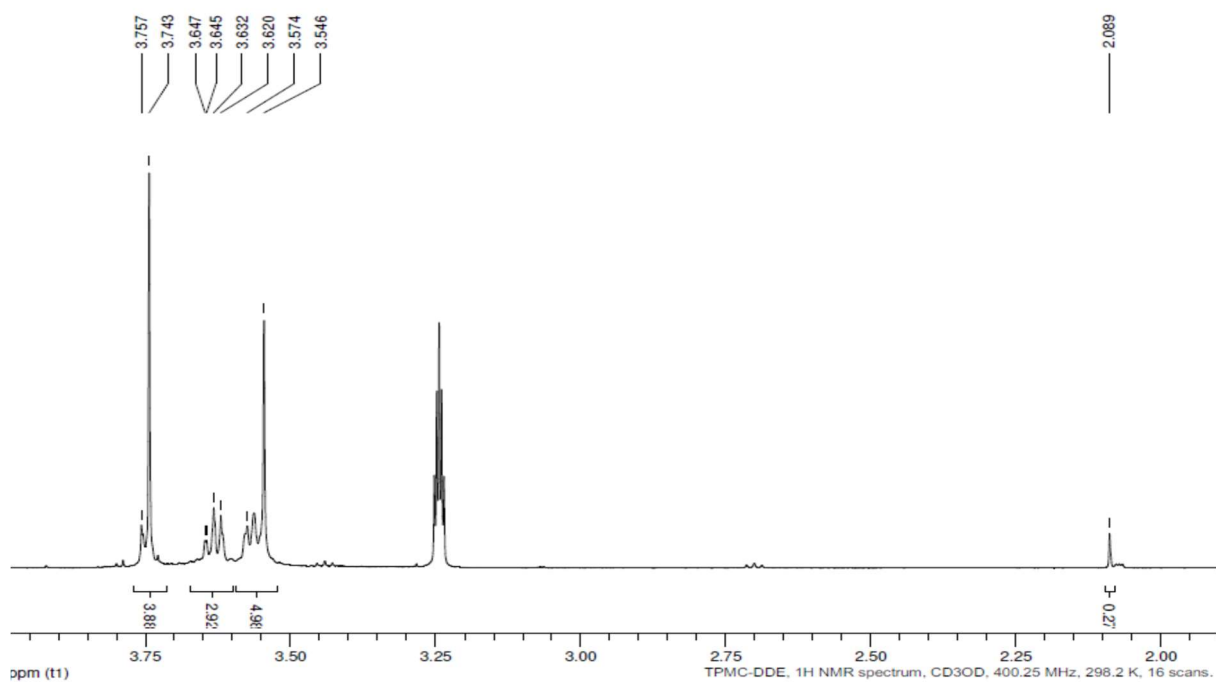


Appendix 5: Experimental ¹H NMR Spectra of TPMC/DDE



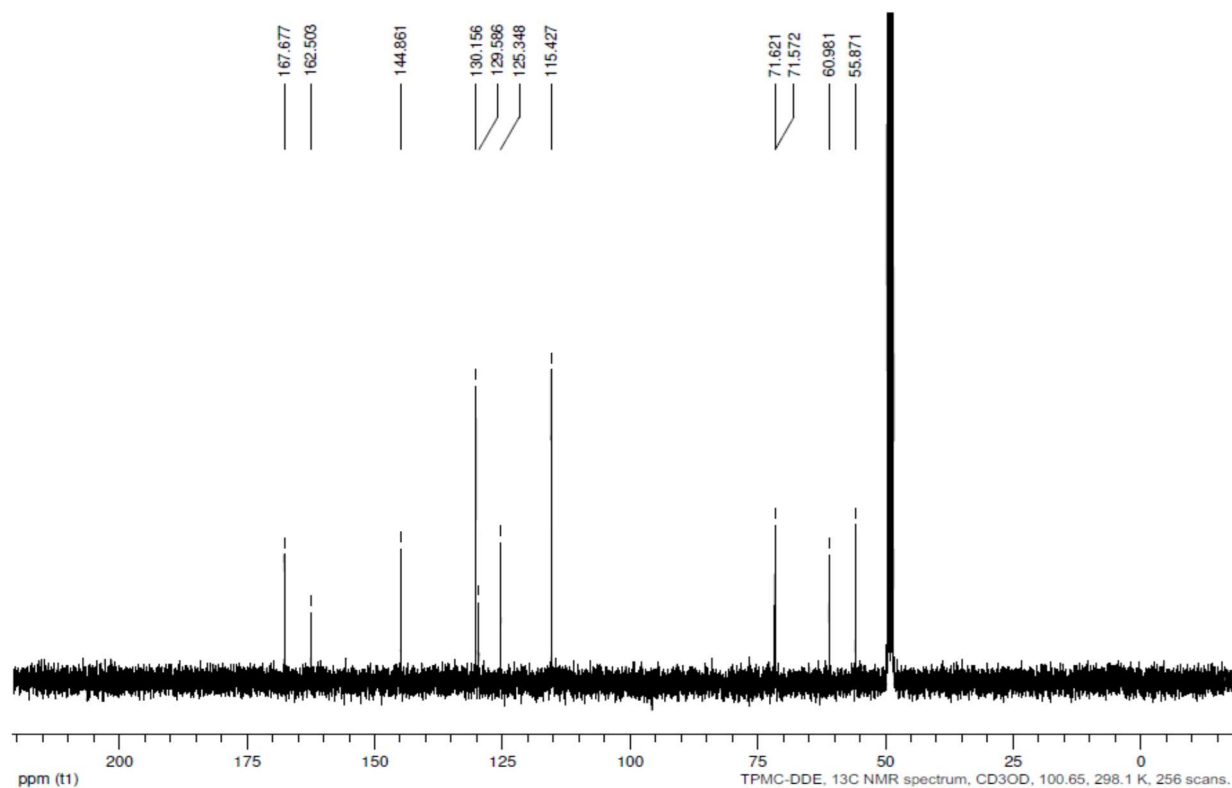


Appendix 5 (a): Experimental ¹H NMR Spectra of TPMC/DDE showing peaks 6.624 – 7.944 ppm

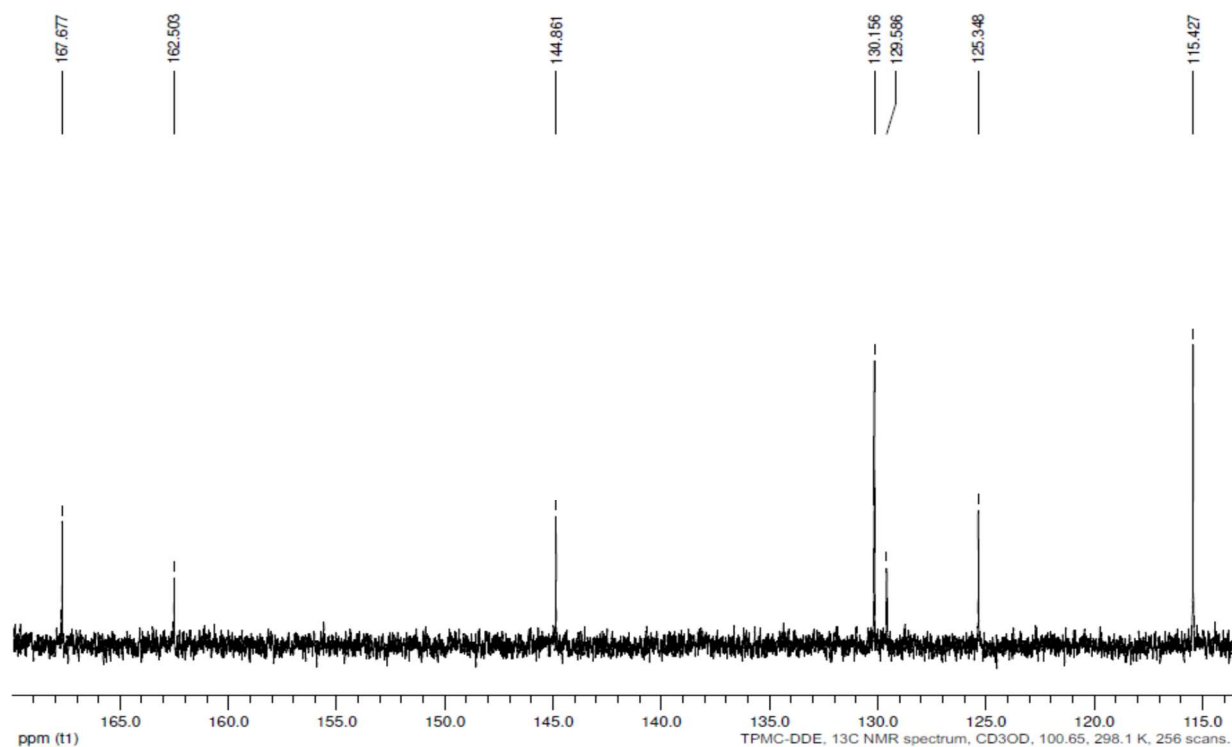


Appendix 5 (b): Experimental ¹H NMR Spectra of TPMC/DDE showing peaks 2.089 – 3.757 ppm



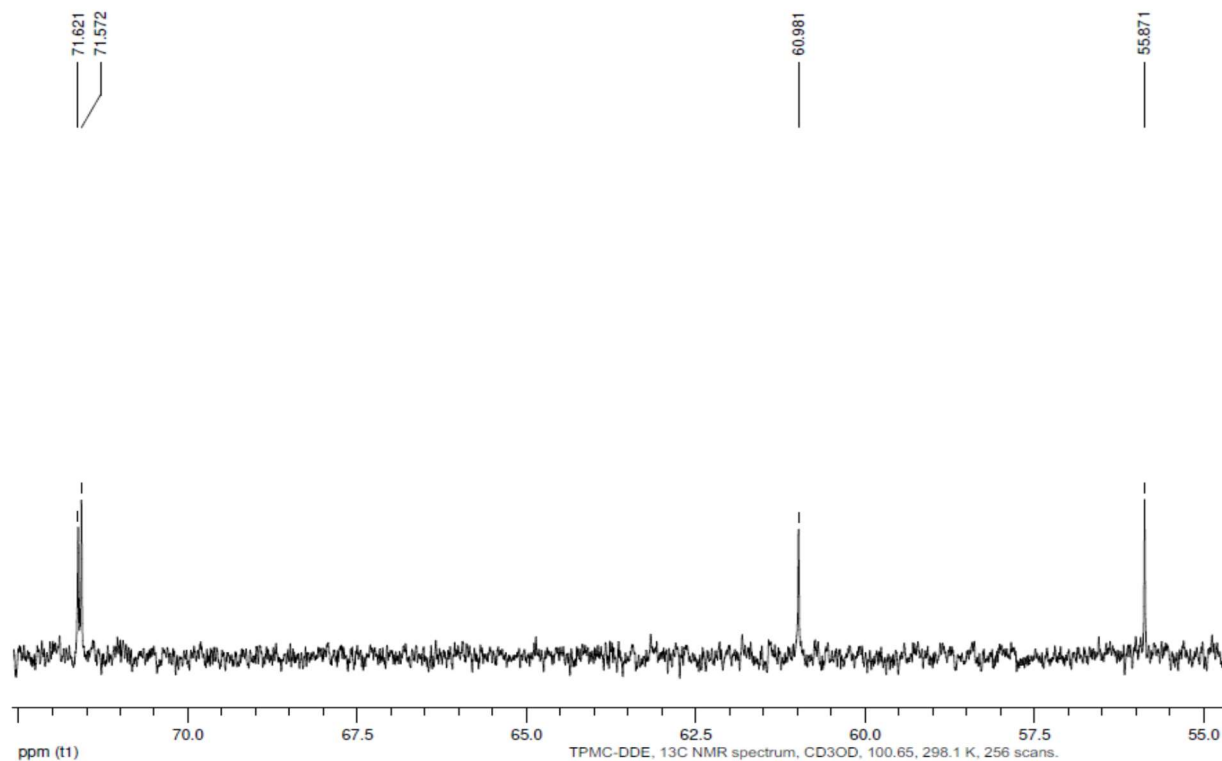


Appendix 6: Experimental ¹³C NMR Spectra of TPMC/DDE



Appendix 6 (a): Experimental ¹³C NMR Spectra of TPMC/DDE showing peaks 115.427- 167.677 ppm





Appendix 6 (b): Experimental ¹³C NMR Spectra of TPMC/DDE showing peaks 55.871- 711.621 ppm

